QUANTIFICATION AND CONTROL OF

ULTRASOUND-MEDIATED CELL DEATH MODES

A Thesis
Presented to
The Academic Faculty

By

Joshua Daniel Hutcheson

In Partial Fulfillment
of the Requirements for the Degree
Master of Science in
Chemical and Biomolecular Engineering

Georgia Institute of Technology

August 2008

QUANTIFICATION AND CONTROL OF

ULTRASOUND-MEDIATED CELL DEATH MODES

Approved By:

Mark Prausnitz, PhD
School of Chemical and Biomolecular Engineering
Georgia Institute of Technology

Athanassios Sambanis, PhD
School of Chemical and Biomolecular Engineering
Georgia Institute of Technology

Andreas Bommarius, PhD
School of Chemical and Biomolecular Engineering
Georgia Institute of Technology

Christopher Jones, PhD
School of Chemical and Biomolecular Engineering
Georgia Institute of Technology

Date Approved: March 10, 2008

Acknowledgements

Let me preface this section by stating that I could write a document as long as this whole thesis and still not fully cover the depth of my gratitude to all of those who have helped me reach this point in my life. I want to begin by thanking my family and friends. My mom and dad have always been my greatest supporters and have taught me more valuable lessons than I have ever learned through my 20 years in school. My little sister is my best friend and always makes me laugh. My grandparents have always made sure that I am well-fed and that I have "a little spending money." I would also like to thank all of my aunts, uncles, cousins, school friends, church friends, and family friends. No one knows how to have as much fun as my family and friends, and I'm thankful for all of the times y'all (I think my southern vernacular is appropriate in this section) have forced me to "loosen up" and "have some fun." Y'all have taught me how to love and be loved, and for that, I love all of you.

I would next like to thank my advisor and everyone associated with the Prausnitz lab and the IBB for all of the advice and support. Working with all of you has been educational and enjoyable. I have learned an incredible amount about research and about myself during my time in the lab. All of you have become more than colleagues, you are also friends (see the previous paragraph). Finally, this work was supported by the National Institutes of Health and the United States Department of Education GAANN program.

Table of Contents

List of Tables

List of Figures

Summary

Ultrasound has been identified as a possible non-invasive drug delivery device that could avoid many of the problems found in traditional therapeutics. Studies have shown that ultrasound can deliver molecules into cells; however, the applicability of ultrasound has been limited due to uncontrollable cellular viability losses after sonication. In this study, we sought to quantify the heterogeneous bioeffects of ultrasound in order to gain more insight into how ultrasound affects cells. We were also concerned with identifying the causes of and preventing programmed cell death caused by ultrasound exposure. In order to accomplish these objectives, we used flow cytometry to group cells into quantifiable characteristic populations. This allowed us to identify the relative importance of different forms of rapid cell death. We found that up to 65% of cells (at the highest ultrasound pressure studied) can lose viability rapidly and, for the first time, quantified them among three distinct populations: (1) cells that retain normal size but lose plasma membrane integrity; (2) intact nuclei surrounded by plasma membrane remnants; (3) debris resulting from cellular lysis. Our analysis was supported by mechanical sorting of these populations and subsequent imaging using confocal microscopy. We then monitored the viable populations for 6 h after ultrasound exposure. Results indicated that up to 15% of viable cells (at the highest ultrasound pressure studied) underwent apoptosis, which we showed was associated with an influx of intracellular Ca^{2+};

therefore, we developed a method of chelating intracellular Ca^{2+} after sonication in an effort to maintain viability of those cells. Using this technique, we showed for the first time that cells could be saved, and we were able to prevent apoptosis by 50%, thereby increasing the overall viability of cells exposed to ultrasound. We conclude that ultrasound is a useful method to deliver molecules into cells and that appropriate selection of sonication conditions can minimize cell death by rapid and apoptotic mechanisms.

Chapter I

Introduction

1.1 Introduction to Intracellular Drug Delivery

Along with advances in medicine and pharmaceutical technologies, research into targeted drug delivery modalities has increased steadily over the last several decades. Patient treatment options are often limited not by the availability of drug and biological therapeutics, but by the ability to deliver a drug to a desired location within the body while avoiding side-effects caused by drug interaction with unintended targets (Langer 1998). The ultimate target of many therapeutics is inside specific cells where a drug can alter cellular biochemistry to achieve a desirable action (Ariuens and Simonis 1964). Unfortunately, most current drug delivery routes lack the ability to target a particular site and rely on the natural action of the body to deliver drugs to cells. This results in drugs inadvertently reaching other cells and tissues or being destroyed by bodily clearance mechanisms. For example, many chemotherapeutics are successful in treating cancerous cells; however, a lack of specificity usually results in a weakened immune system and other dangerous side-effects that can be harmful to a patient (Love, Leventhal et al. 1989).

A variety of studies have been done to overcome the delivery problems associated with traditional therapeutics. Electroporation was one of the earliest

identified physical methods to disrupt cellular membranes (Tsong 1991). Using this technique, a voltage is applied across cell membranes, resulting in the formation of transient nanometer pores through which drugs and small molecules can pass (Canatella, Black et al. 2004). While electroporation shows the ability to effectively deliver molecules into cells, it often involves high voltages and cannot easily reach many tissues within the body (Weaver 1993).

The advent of new therapeutics composed of DNA, RNA, and proteins has brought even more challenges to the field of drug delivery (Pouton and Seymour 2001). Gene gun therapies use particle bombardment to deliver DNA into cellular targets but have limitations due to high cost and poor control (Cupp and Bloom 2002). The use of viruses has also been identified as a potential carrier and intracellular delivery vehicle for genetic material; however, the infectious and immunological nature of viruses has raised many concerns over their accepted use for targeted delivery (Cupp and Bloom 2002).

An ideal drug delivery system would allow the delivery of a large variety of therapeutic molecules to a specific target site in a minimally invasive and cost effective manner. The major benefit of a targeted therapeutic system is that overall dosage requirements can be lowered by allowing little to no therapeutic losses from drug interaction with non-targeted tissues (Langer 1998). This makes treatments safer and more efficient for the patient. To accomplish this task, a delivery system should be predictable and controllable to ensure that the intended target cells and tissues are reached.

Due to its accepted use as a noninvasive, yet targeted, diagnostic tool, ultrasound has been identified as a possible system to achieve this kind of drug delivery. At intensities higher than those used in diagnostics, ultrasonically-induced cavitation has been shown to reversibly disrupt the plasma membranes of cells (Cochran and Prausnitz 2001; Guzman, Nguyen et al. 2001; Ogawa, Tachibana et al. 2001; Tang, Wang et al. 2002; Schlicher, Radhakrishna et al. 2006; Gac, Zwaan et al. 2007)—the main barrier to intracellular drug delivery. Studies have shown the ability of ultrasound to deliver small molecules (Keyhani, Guzman et al. 2001; Guzman, Nguyen et al. 2002; Ng and Liu 2002), large dextrans (Schlicher, Radhakrishna et al. 2006), and DNA (Duvshani-Eshet and Machluf 2005; Paliwal and Mitragotri 2006; Zarnitsyn, Kamaev et al. 2007) into cells in vitro. Other studies have also shown that ultrasound can effectively target cellular sites in ex vivo tissues (Hallow, Mahajan et al. 2007) and in vivo animal models (Bednarski, Lee et al. 1997).

Ultrasound fulfills the therapeutic requirements of being easily targeted, minimally invasive, and cost effective; however, it has not been realized as a clinical tool due to a lack of predictability and controllability (Guzman, Nguyen et al. 2001). Studies have indicated that increasing intracellular delivery of molecules using ultrasound comes at a cost of lost cellular viability (Miller, Miller et al. 1996; Guzman, Nguyen et al. 2001; Keyhani, Guzman et al. 2001; ter Haar 2007). Moreover, both the level of intracellular uptake (Guzman, Nguyen et al. 2001; Keyhani, Guzman et al. 2001; Guzman, Nguyen et al. 2002) and types of viability loss (Guzman, Nguyen et al. 2001; Guzman, McNamara et al. 2003) are

heterogeneous and difficult to control. In this study, we will seek to characterize and quantify the relative importance of ultrasound-induced bioeffects. We will also discuss methods to control ultrasound-mediated viability loss.

1.2 Objectives

The objectives of this study are as follows:

1) Characterize and quantify ultrasound-mediated bioeffects
2) Identify causality of ultrasound-induced programmed cell death
3) Prevent programmed cell death using intervention strategies

1.3 Overview of the Thesis

This chapter provides an introduction to targeted drug delivery in general and gives a brief overview of ultrasound-mediated drug delivery. Chapter 2 establishes the relevance of the study and provides background on the physical characteristics of ultrasound and cavitation, ultrasound-induced bioeffects, and important aspects of cellular biochemistry. The materials and methods used in this study are described in chapter 3. Chapter 4 will give results of quantification and characterization of the short-term effects of ultrasound; whereas, chapter 5 will look at the downstream cellular effects caused by ultrasound as well as means to prevent undesired cellular responses. The two results sections will be discussed in chapter 6, followed by concluding remarks given in chapter 7. Finally, chapter 8 will offer recommendations for future studies.

Chapter II

Background

2.1 Motivation of Study

As mentioned previously, the plasma membrane is the primary barrier to drug delivery into cells and tissues. The effectiveness of this barrier can be found in the structure of the plasma membrane (McNeil and Steinhardt 1997; Ko and McCulloch 2000; Vlahakis and Hubmayr 2000; Morris and Homann 2001). It is composed of a bilayer with hydrophobic lipid domains between hydrophilic head groups that face the extracellular environment and the intracellular cytosol. This bilayer creates a boundary around the cell that severely limits the types of molecules that can pass into and out of the cell (McNeil and Steinhardt 1997). These limitations have proven to be major problems for new cellular therapeutics that are based on the delivery of genetic material or proteins into cells (Pouton and Seymour 2001).

Ultrasound has been identified as a possible means to overcome the barrier posed by the plasma membrane. At high ultrasound pressures, cavitation has been shown to reversibly permeabilize plasma membranes, allowing molecules to be delivered into cells (Schlicher, Radhakrishna et al. 2006). Ultrasound is an attractive candidate for targeted drug delivery because it is minimally invasive, inexpensive, and well-accepted as a clinical diagnostic tool (Ng and Liu 2002).

However, it has suffered from a lack of controllability that is characterized by large losses of cellular viability. An increase in ultrasound pressure generally leads to more molecules delivered to cells but also causes more cells to lose viability (Guzman, Nguyen et al. 2001). Cells have even been observed to lose viability hours after sonication has ended (Ashush, Rozenszajn et al. 2000; Vykhodtseva, McDannold et al. 2001; Lagneaux, de Meulenaer et al. 2002; Honda, Kondo et al. 2004; Feril, Kondo et al. 2005).

In this study we seek to characterize and quantify the various bioeffects caused by ultrasound. We would then like to look at the key factors in cellular viability loss that occurs hours after ultrasound exposure and offer methods to prevent this type of cell death. First, however, we will give some background on both the physical aspects of ultrasound and the biological response of the cells.

2.2 Properties of Ultrasound

Ultrasound is defined as any frequency of sound greater than 20 kHz, the maximum sound frequency that humans can hear (Leighton 2007). Higher ultrasound frequencies provide a smaller focus, and thus, give better targeting and finer resolution. Therefore, ultrasound frequencies for diagnostic procedures range from 1 – 30 MHz; whereas, therapeutic procedures tend to use lower ultrasonic frequencies ranging from 21 kHz – 5 MHz (Postema and Gilja 2007). For this study, an ultrasound frequency of 24 kHz was used. Lower frequencies require less energy to induce cavitation (Leighton 2007), the driving force behind ultrasound-mediated drug delivery.

In the context of ultrasound, cavitation is defined as the rapid formation and oscillation of microbubbles. At a threshold peak pressure based on the ultrasound frequency, microbubbles are formed when dissolved gases nucleate in a liquid medium to form gas bubbles surrounded by liquid (Leighton 2007). An increase in ultrasound energy has been shown to cause an increase in the number of microbubbles formed, as measure by cavitation (Cochran and Prausnitz 2001). For higher frequencies, the pressure required for microbubble nucleation is high; therefore, contrast agents, gas bubbles encapsulated by a solid shell, are often used to provide nucleation sites (Dalecki, Raeman et al. 1997; Kamaev, Hutcheson et al. 2004). The oscillation of microbubbles can either be stable, where the bubbles oscillate with the characteristic harmonics and subharmonics of the ultrasound wave, or inertial, where the bubbles reach critical radii during nonlinear oscillations and then collapse violently (Lauterborn and Ohl 1997). The intense shear energy released from inertial cavitation is believed to cause ultrasound-induced bioeffects (Miller, Miller et al. 1996; Cochran and Prausnitz 2001).

Important Terms

- Frequency: the number of cycles in a given period of time
- Pulse length: time of one pulse of acoustic energy
- Duty cycle: the percentage of time that the transducer produces acoustic waves during the total time of ultrasound exposure
- Exposure time: the duty cycle multiplied by the total time of ultrasound exposure

- Ultrasound pressure: the peak pressure of the acoustic waves
- Acoustic energy: a function of the square of the ultrasound pressure multiplied by the exposure time
- Cavitation: the formation and subsequent oscillation of microbubbles

2.3 Ultrasound-Induced Bioeffects

Ultrasound has great potential as a clinical therapeutic tool; however, its use has been hampered by the lack of predictability and controllability resulting from heterogeneity of ultrasonically-induced bioeffects (Barnett, ter Haar et al. 1994; Guzman, Nguyen et al. 2001; Dalecki 2004). Previous studies have identified a myriad of cellular bioeffects resulting from sonication. Our lab (Guzman, Nguyen et al. 2002) has previously shown that small macromolecules can be loaded into cells at equilibrium levels; the amount of loading strongly depends on the applied ultrasound conditions. Others have shown that larger molecules, such as high molecular weight dextrans, can be delivered into cells with the amount of delivery dependent upon the size of the molecule (Schlicher, Radhakrishna et al. 2006). Many researchers have built upon this foundation to use ultrasound to deliver chemotherapeutics and other drugs to cells and tissues in vitro (Husseini, El-Fayoumi et al. 2000; Marin, Sun et al. 2002; Rosenthal, Sostaric et al. 2004; Zarnitsyn, Kamaev et al. 2007).

With the advent of protein and gene therapies, ultrasound has received a significant amount of attention as a potential delivery device (Duvshani-Eshet, Baruch et al. 2006; Paliwal and Mitragotri 2006; Campbell and Prausnitz 2007;

Zarnitsyn, Kamaev et al. 2007). Studies have shown that the plasma membrane breaks caused by ultrasound are large enough to deliver DNA plasmids into cellular cytosol (Mehier-Humbert, Bettinger et al. 2005; Duvshani-Eshet, Baruch et al. 2006) and that ultrasound can facilitate transfection in treated cells (Ogawa, Kagiya et al. 2004). Similar studies have shown that ultrasound can also deliver proteins and RNA into cells (Kinoshita and Hynynen 2005). The delivery of these macromolecules indicates that ultrasound can create large plasma membrane disruptions that can be repaired by cells. This wound-mediated delivery mechanism was supported by experiments performed by Schlicher et. al. (Schlicher, Radhakrishna et al. 2006) in which cellular endocytosis was blocked but ultrasound-induced intracellular delivery was still observed. Also, when cellular repair pathways were disrupted, cells were not able to recover from ultrasound exposure. Furthermore, microscopy analyses revealed that plasma membrane disruptions that lead to uptake of extracellular molecules could be up to microns in diameter; however, many cells are unable to recover from these disruptions.

At high acoustic energies, where molecular loading is the highest, cell viability drops dramatically (Cochran and Prausnitz 2001; Guzman, Nguyen et al. 2001; Keyhani, Guzman et al. 2001). The loss of cell viability observed within 30 min post-sonication has been attributed to cell lysis (Carstensen, Kelly et al. 1993; Miller and Quddus 2001; Feril, Kondo et al. 2004) and uncontrolled death modes from irreparable wounds to the plasma membrane (Schlicher, Hutcheson et al. 2007). These modes of cell death have been correlated to increased

inertial cavitation as monitored by acoustic spectra recordings (Cochran and Prausnitz 2001) and contrast agent destruction (Kamaev, Hutcheson et al. 2004). The inherent heterogeneity of ultrasound that results in both rapid cell death from irreparable plasma membrane wounds and recoverable wounds that lead to intracellular uptake has been hypothesized to be a function of cellular distance from the site of microbubble collapse (Guzman, McNamara et al. 2003; Sundaram, Mellein et al. 2003). Cells closest to the inertial cavitation event are completely lysed; whereas, at some distance away from the implosion, cells are not affected.

Recent studies have shown that ultrasound treatment can also cause cells to undergo a controlled type of cell death, apoptosis, hours after sonication (Ashush, Rozenszajn et al. 2000; Vykhodtseva, McDannold et al. 2001; Lagneaux, de Meulenaer et al. 2002; Honda, Kondo et al. 2004; Feril, Kondo et al. 2005). Honda, et al. (Honda, Kondo et al. 2004) attributed ultrasound-induced apoptosis in lymphoma cells to an increase in cytosolic Ca^{2+}. This was hypothesized to be caused by a large influx of external Ca^{2+} ions across the plasma membrane; however, attempts to save apoptotic cells by chelating intracellular Ca^{2+} resulted in an increase in uncontrolled, necrotic cell death. Others have suggested that reactive oxygen species (ROS) that are formed by cavitation could also play a role in long-term cell death (Lagneaux, de Meulenaer et al. 2002), but follow-up studies have shown that these ROS are very short-lived (Honda, Zhao et al. 2002; Feril, Kondo et al. 2005) and that treatments with

antioxidants fail to inhibit ultrasound-mediated apoptosis (Honda, Kondo et al. 2004).

All of the ultrasound-mediated bioeffects listed above (i.e. uptake, rapid viability loss, and delayed viability loss) can be broadly grouped into four categories: (1) cells that appear largely unaffected, (2) cells reversibly permeabilized, as evidenced by intracellular uptake of molecules, and that remain viable, (3) cells rendered nonviable during sonication, as shown by an irreversible loss of the plasma membrane barrier or lysis of the cell into debris and (4) cells that appear to be viable shortly after sonication, but later undergo apoptosis and die. Applications of ultrasound often seek to maximize the second population, in order to achieve intracellular drug or gene delivery, and minimize the third and fourth populations, since cell death is generally undesirable.

2.4 Cellular Wounding and Repair

Since ultrasound delivers molecules into cells by disrupting plasma membranes, it is important to understand how cells respond to membrane wounds. As discussed above, the plasma membrane carefully regulates the movement of molecules into and out of a cell. When this barrier is disrupted, molecules move freely across the plasma membrane to establish a concentration equilibrium between the intracellular and extracellular environments. This transport allows ultrasound to deliver molecules into cells; however, the lost membrane integrity and loss of normal intracellular ion concentrations can be detrimental to the cell (Nicotera, Bellomo et al. 1990; Trump and Berezesky 1995). To maintain normal cellular functions, the cell must act quickly to repair

disruptions. This repair process can be complex and energy intensive (McNeil and Steinhardt 1997; McNeil, Vogel et al. 2000).

Cells in normal homeostasis maintain a lower concentration of intracellular Ca^{2+} ions than that of the external cellular environment (Trump and Berezesky 1992; Berridge, Bootman et al. 1998; Nguyen, Bittner et al. 2005). When the ultrasonically-induced cavitation disrupts plasma membranes of cells, the natural concentration gradient causes extracellular Ca^{2+} ions to rush into cells. This ion movement is necessary in wounded cells because Ca^{2+} is an initiator and messenger in biochemical plasma membrane wound repair pathways (Zamansky, Nguyen et al. 1991; Rettig and Neher 2002; McNeil, Miyake et al. 2003; Meldolesi 2003; McNeil and Kirchhausen 2005). At a sufficiently high concentration, Ca^{2+} ion binding to cytosolic proteins triggers a biochemical cascade that results in the recruitment of lipid repair vesicles to the site of plasma membrane wounding (Terasaki, Miyake et al. 1997; McNeil and Kirchhausen 2005). These vesicles can then fuse to create a patch to seal the plasma membrane disruption. However, at cytosolic concentrations higher than physiologic levels, Ca^{2+} can also initiate programmed cell death pathways (Trump and Berezesky 1992; Nicotera and Orrenius 1998; Burek, Burek et al. 2003; Orrenius, Zhivotovsky et al. 2003).

2.5 Cellular Death

For the purposes of this study, we will discuss the two most common forms of cell death, necrosis and apoptosis. Uncontrolled, or necrotic, cell death is commonly defined as an accidental form of cell death resulting from a

disruption of normal cellular functions (Trump, Berezesky et al. 1997; Tsujimoto 1997). As used in this context, this mode of cell death can broadly encompass cellular lysis and more controlled forms of necrosis (Kroemer, Dallaporta et al. 1998; Kitanaka and Kuchino 1999; Proskuryakov, Gabai et al. 2002). The most important aspect of cellular necrosis is that the death was not a result of an active cellular process, but rather a consequence of a traumatic cellular event that resulted in the loss of plasma membrane integrity. This usually results in cytosolic contents spilling into the extracellular environment, which leads to large inflammatory responses in the body (Edinger and Thompson 2004).

On the other hand, apoptosis, or programmed cell death, is a controlled form of cell death that occurs in many normal physiological situations (Bohm and Schild 2003). Many apoptotic pathways have been elucidated, and the cascades of enzymes that lead to cell death can be complex (Tsujimoto 1997; Fadeel, Zhivotovsky et al. 1999; Bohm and Schild 2003). During the progression of apoptosis the cell membrane remains mainly intact while the nuclear envelope is broken and the DNA of the cell is degraded. The cell then forms small apoptotic bodies that consist of a plasma membrane bilayer surrounding damaged organelles and DNA fragments (Bohm and Schild 2003). In the body, these bodies are engulfed by macrophages, thus limiting the inflammatory response associated with necrosis.

2.6 Relevance of Work

The goal of this study was first to quantify the fraction of cells in each of these populations shortly after sonication and as a function of time for up to 6 h

after sonication. In this way, we sought to determine which cells from among the initial populations ultimately become the apoptotic cells described in previous studies. Based on this information, our second goal was to determine why those cells became apoptotic and to develop a strategy to reverse the effect and keep those cells alive. We must also identify time frames within which intervention strategies can be implemented. If successful, this strategy could facilitate drug and gene deliveries using ultrasound by keeping more cells viable. Finally, we present results demonstrating methods to control bioeffects.

Chapter III

Materials and Methods

3.1 Cell culture

DU 145 prostate-cancer cells (American Type Culture Collection, Manassas, VA) were grown to 80 – 90% confluence on T-150 flasks (BD Falcon, Franklin Lakes, NJ) in cellular growth media (RPMI-1640, Cellgro, Herndon, VA) that was supplemented with 10% fetal bovine serum (Atlanta Biologicals, Atlanta, GA) at 37ºC, 5% CO_2, and 90% relative humidity. The cells were harvested from the flasks by trypsinization using previously described protocols (Guzman, Nguyen et al. 2001).

3.2 Ultrasound apparatus

The ultrasound apparatus consisted of a cylindrical piezoelectric transducer (Channel Industries, Santa Barbara, CA) sealed between two PVC pipes (5.1 cm inner diameter), as described previously (Cochran and Prausnitz 2001). This chamber was filled with deionized water that was degassed for at least 2 h in a bell jar (Nalgene, Rochester, NY) using a vacuum pump (KNF Neuberger, Trenton, NJ) to reduce cavitation in the water bath surrounding the cellular samples.

Ultrasound was generated at 24 kHz by a function generator (DS354 SRI, Stanford Research Systems, Sunnyvale, CA). The pulsed signal was sent to an amplifier (Macro-Tech 2410, Crown Audio, Elkhart, IN) that controlled the transducer via a matching transformer (MT-56R, Krohn-Hite, Avon, MA). Using this system, the frequency, duty cycle, incident pressure, and pulse length were set. The exposure time was controlled manually. The peak ultrasound pressure was found using a calibrated hydrophone (Reson, Goleta, California), which gave a relationship of P[atm] = 0.0089V, where V is the voltage applied to the transducer. Samples were exposed at room temperature to 20 acoustic pulses at a duty cycle of 10% at 24 kHz. Each pulse applied ultrasound at a peak pressure of either 3.6 atm or 5.3 atm for a 0.1 s pulse length. Sham exposure samples (non-sonicated controls) samples were prepared identically to the sonicated samples, but no ultrasound was applied (Guzman, Nguyen et al. 2001). An image of the overall ultrasound setup is shown in Figure 1a. A close-up image of the transducer is shown in Figure 1b.

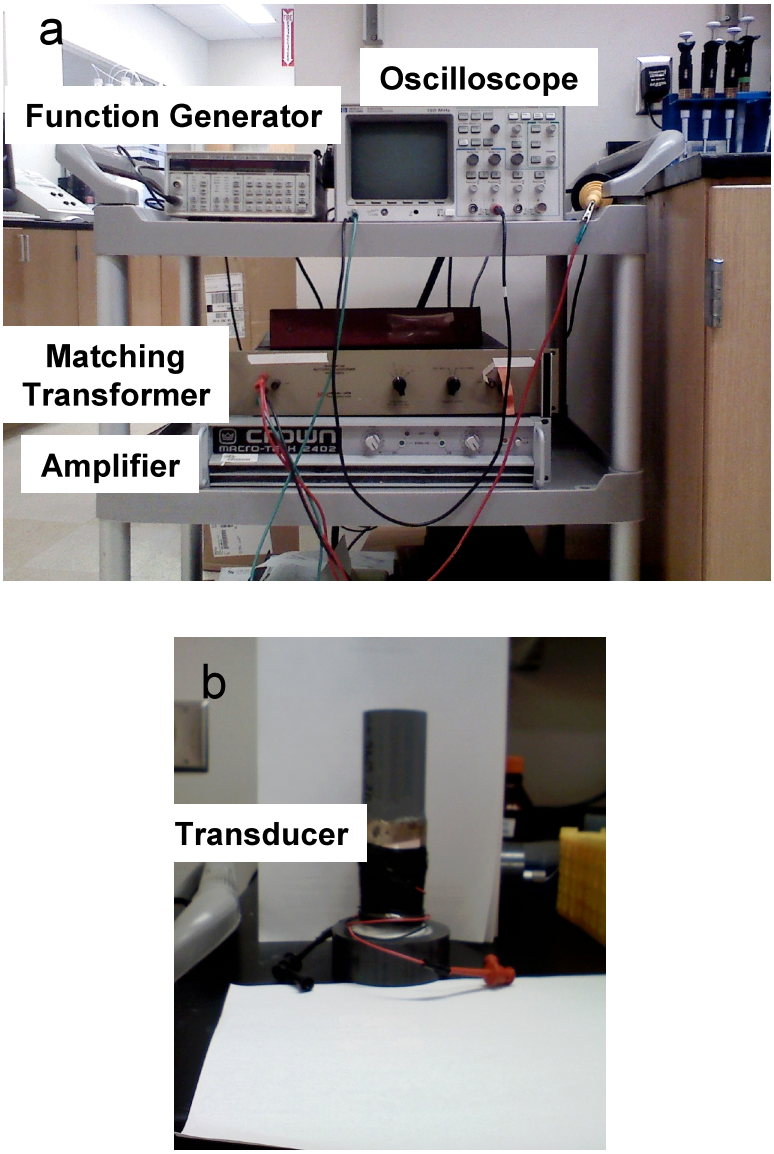

Figure 1. Ultrasound system used in this study. (a) A ultrasound wave of 24 kHz is produced by a function generator, amplified, and sent to the transducer via a matching transformer. (b) The transducer is set between two pvc pipes, creating a water-tight bath.

3.3 Ultrasound exposure

Following established protocols (Cochran and Prausnitz 2001), well-mixed cell suspensions at a concentration of 10^6 cells/ml in growth media were introduced into 1.2 ml sample chambers (No. 241 SEDI-PET SAMCO, San Fernando, CA transfer pipets using a 22-gauge needle and 3-ml syringe (Becton-

Dickinson, Franklin Lakes, NJ). After the chamber was filled, a stainless steel rod (1.6 mm diameter) was inserted into the pipet stem to seal the chamber and provide a means to suspend the chamber in the water bath. Sample chambers were then positioned in the exposure chamber water bath by fixing the end of the suspending rod into the chamber cover at a location that positioned the sample chamber in the axial and radial center of the transducer (Cochran and Prausnitz 2001).

3.4 Quantification of Intracellular Uptake

To study uptake, cells were sonicated in RPMI-1640 (with serum) in the presence of either 10 μM calcein (Invitrogen, Carlsbad, CA), a plasma membrane impermeant green-fluorescent marker or 10 μM sulforhodamine 101 (Invitrogen), a plasma membrane impermeant red-fluorescent marker. After exposure, samples were allowed to recover from the effects of sonication for 10 min at room temperature and then spun down at room temperature for 6 min at 1000 x g to remove excess label from the extracellular medium, followed by washing at least twice in phosphate-buffered saline (PBS, Cellgro) and then assayed via flow cytometry, as described below. To determine the amount of intracellular calcein uptake in terms of molecules per cell, FITC-calibration beads were used as described by Guzman, et. al. (Guzman, Nguyen et al. 2001).

3.5 Quantification of Cellular Viability

Propidium iodide (PI) (Invitrogen Corp., Carlsbad, CA) exclusion indicates an intact cellular membrane and is often used to test for cellular viability. When a cellular membrane has been compromised, PI can enter the cell and bind to the cellular DNA. This binding is detected by the red fluorescence emitted by PI. To determine cellular viability, 7.5 μM PI was added to cell samples at least 5 min prior to assaying via flow cytometry. PI exhibits fluorescence only when bound to cellular DNA; therefore, excess PI did not need to be washed from the extracellular media.

Many cells are lysed by sonication, and thus undetected as whole cells by the flow cytometer; therefore, the gated total cells of all sonicated samples were normalized to the gated total cells in the control, sham-exposure samples. The control samples were assumed to have no cellular debris. This assumption ensures that all of the quantified cellular lysis resulted from the actual sonication. The quantification of debris was done by recording the amount of time required to collect 30000 cells in each sample. Since the cells lost due to lysis resulted in a longer required collection time for sonicated samples (i.e. the sonicated samples have a lower cell concentration), the amount of lost cells was calculated as the balance of cells that would be required for the sonicated samples to have the same flow cytometry collection time as the control samples.

3.6 Determination of Intracellular Ca^{2+}

Fluo-4 AM (Invitrogen Corp., Carlsbad, CA) fluoresces upon binding to Ca^{2+} in live cells. By measuring the intensity of the fluo-4 fluorescence using flow

cytometry, cells with increased intracellular Ca^{2+} can be identified. For cellular loading, fluo-4 AM was dissolved in dimethyl sulfoxide (Sigma-Aldrich, St. Louis, MO) at a concentration of 5 mM and added to cellular samples following ultrasound exposure and a post-sonication incubation time specified in the results at a final concentration of 5 μM. To assay intracellular Ca^{2+} levels, samples were incubated in the presence of fluo-4 AM at room temperature for 30 min, washed once in PBS, and then assayed via flow cytometry.

3.7 Annexin V Apoptosis Protocol

One of the first identifiable events in the cascade of apoptosis is the translocation of phosphatidyl serine to the outer leaflet of the plasma membrane in intact cells. In the body, this translocation signals the recruitment of macrophages to remove cellular remnants post-apoptosis. Fluorescently-conjugated annexin V (Invitrogen Corp., Carlsbad, CA) molecules bind to phosphatidyl serine, allowing early apoptotic cells to be identified using flow cytometry. In the early stages of apoptosis, the plasma membrane of the cell remains intact; therefore, early apoptotic cells are differentiated from necrotic cells by PI exclusion, similar to the method described for the quantification of cellular populations. Late stage apoptosis, or secondary necrotic cells, cannot be identified in this manner. However, they are usually smaller and lose DNA due to the formation of apoptotic bodies. At the time-points for this study, these characteristics were not observed; therefore, this study only considers early apoptosis.

After sonication, cells were incubated for (i) 4 to 24 h at 37 ^{o}C or (ii) up to 2 h at room temperature. The cells were then suspended in annexin-binding buffer (prepared using standard manufacturer protocols) and incubated with 5 µl FITC-conjugated annexin V stock solution (Invitrogen) per 100 µl cell suspension. Each sample was analyzed via flow cytometry after 15 min of incubation at room temperature.

3.8 Ca^{2+} Chelation via BAPTA AM

BAPTA, AM (Sigma-Aldrich, St. Louis, MO) is often used as a Ca^{2+} chelator in live cells. BAPTA is similar in structure to and function of EGTA, but is less sensitive to changes in pH. By adding an acetoxylmethyl (AM) ester group, the chelating action of BAPTA is inhibited until the molecule is cleaved by intracellular esterases. These factors make BAPTA, AM suitable for intracellular Ca^{2+} chelation. For chelation, a stock solution BAPTA, AM in dimethyl sulfoxide was added to appropriate cellular suspensions 1 min after sonication at a final concentration of 130 µM. Cells were incubated with BAPTA AM at room temperature for 30 min and then centrifuged to remove extracellular dimethyl sulfoxide. Samples were then prepared according to protocol for the specified assay.

3.9 Flow Cytometric Analysis

Samples were run on a BD-LSR flow cytometer using FACS DiVa software (BD Biosciences, Franklin Lakes, NJ) based on previously established

methods (Guzman, Nguyen et al. 2001). Relative cellular size was obtained through measurement of the light scattering properties of the cells as detected by forward scatter (FSC) measurements. The fluorescence of green marker compounds (including calcein and Fluo-4 AM) was measured with a 488-nm argon laser excitation and a 530/30 bandpass filter for emission. Red-fluorescent propidium iodide was also excited at 488 nm and measured using a 675/20 nm bandpass filter for emission. For each sample, 30000 events were collected from a gated region known from previous work (Canatella, Karr et al. 2001) to contain DU 145 cells. Data were analyzed using FCS Express (De Novo Software, Thornhill, Ontario) flow cytometry analysis software. Table I shows a breakdown of how the various assay markers were used to identify cellular characteristics.

Table I. Cellular Categorization with Various Assays

	Calcein	**PI**	**Annexin**	**FSC**
Viable, No Uptake	-	-	-	Normal
Viable, Uptake	+	-	-	Normal
Necrotic	-	+	+	Smaller
Early Apoptotic	?	-	+	Normal

Chapter IV

Identification and Quantification of Cellular Populations

4.1 Introduction

Previous studies have quantified how cells shift from viable cell populations before sonication to a distribution of uptake and viable cell populations immediately after sonication (Guzman, Nguyen et al. 2001). However, limited attention has been given to the quantitative distribution among the types of viability loss after ultrasound exposure. This study offers a new analysis for characterizing cells after sonication. We believe that it will give valuable insight into the relative importance of cellular effects.

4.2 Quantification of Viability in Cellular Populations

The first goal of this study was to quantify the fraction of cells among characteristic populations created shortly after sonication. These populations can be distinguished in part by measured cellular forward scatter on the flow cytometer, which is a measure of relative cell size, and propidium iodide (PI) fluorescence, which is a measure of cell viability determined by plasma membrane exclusion of the dye. These measurements were made 15 to 30 min after sonication ended, which is longer than the transient state of membrane

permeability associated with ultrasound (Schlicher, Radhakrishna et al. 2006). Thus, propidium iodide labeling is interpreted as identifying nonviable cells.

As shown in Figure 2a, in the absence of ultrasound, most cells exhibited strong forward scatter and weak propidium iodide fluorescence. This is consistent with a population of intact, viable cells. We have labeled this group of cells as populations 1 and 2 because we do not yet have information on intracellular uptake. Population 1 cells are intact and viable without uptake and Population 2 cells are intact and viable with uptake. In Figure 2a, 98% of cells fell in this category of intact viable cells.

After cells were exposed to sonication, many additional cellular outcomes are evident, as shown in Figure 2b. Some cells (40%) remained in the region of strong forward scatter and weak propidium iodide fluorescence (i.e. intact, viable cells in Populations 1 and 2) after sonication at 3.6 atm. At 5.3 atm of ultrasound pressure, only 28% of cells remained in this population. Other cells exhibited strong PI fluorescence, with either no change in forward scatter (1% at 3.6 atm exposure and 0.5% at 5.3 atm exposure) termed Population 3A or a decrease in forward scatter (45% at 3.6 atm exposure and 58% at 5.3 atm exposure) termed Population 3B. In previous analysis coupling flow cytometry with microscopy (Schlicher, Hutcheson et al. 2007), these cells have been identified as intact, non-viable cells (Population 3A) and wound-derived perikarya, which are cells that have lost cytosol, but retain an intact nucleus in a smaller cell (Population 3B). Other cells have very weak forward scatter and moderate (Population 3C) or weak (Population 3D) PI fluorescence. We previously identified these as

debris from cells lysed during sonication containing nuclear fragments with DNA (Population 3C) or without DNA (Population 3D) (Schlicher, Hutcheson et al. 2007). Since these populations do not correspond to whole cells, they cannot be independently quantified. Therefore, we calculated these cells as the balance of cells no longer counted after sonication. At an ultrasound pressure of 3.6 atm, only 2% of cells fall into this category, but when the pressure is increased to 5.3 atm, these debris populations account for 10% of the total cells.

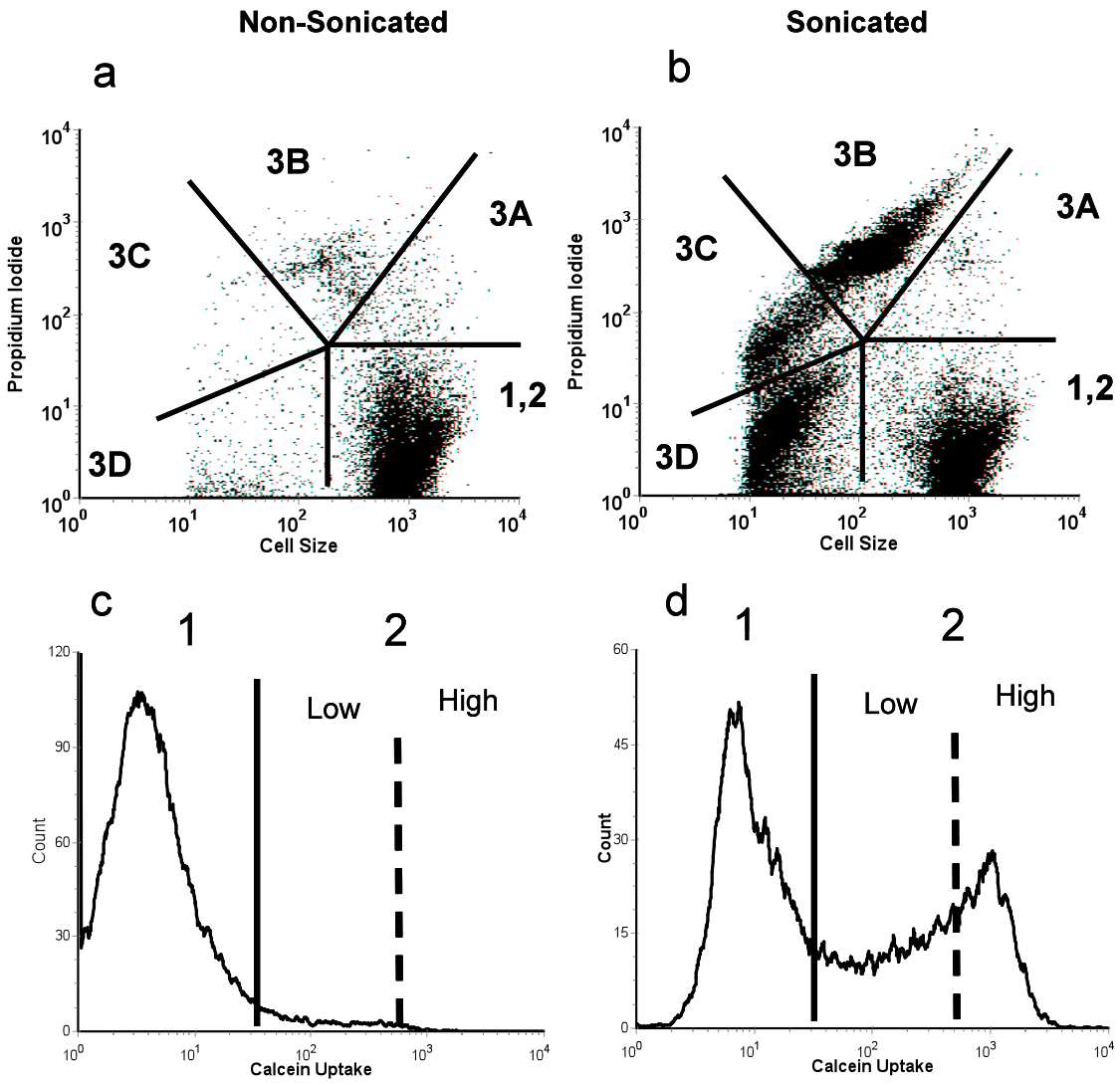

Figure 2. Cellular populations before and after ultrasound exposure. (a) A flow cytometry plot of PI versus cell size for control samples shows cells mainly grouped into Populations 1 and 2. (b) After sonication, cells shift into non-viable populations (Population 3). (c) A histogram of calcein uptake shows background fluorescence in a control sample. (d) Sonicated cells show increased intracellular uptake (Population 2).

4.3 Quantification of Uptake in Viable Cellular Populations

Our analysis so far has distinguished between viable (Populations 1 and 2) and various types of nonviable (Populations 3A-D) cells. Among the viable cells, we next wanted to distinguish between those without uptake (Population 1) and with uptake (Population 2) of calcein, a green fluorescent tracer molecule

that is unable to enter intact cells. In contrast to PI, which was added to cells well after sonication and thereby labeled irreversibly permeabilized (i.e. nonviable) cells, calcein was added prior to sonication, and remained present during sonication. In this way, calcein uptake identifies cells reversibly permeabilized by ultrasound, because cells permitted calcein entry initially and then retained calcein intracellularly during post-sonication washing, which indicates a return of plasma membrane integrity.

In Figures 2c-d, we show the subset of cells analyzed in Figures 1a-b that were intact and viable (Populations 1and 2) as a function of their green fluorescence corresponding to uptake of calcein. As shown in Figure 1c, most cells in the control sample (92% of intact cells) show only background levels of green fluorescence, consistent with normal, non-sonicated cells. The small amount showing signs of intracellular uptake (8% of intact cells) is probably due to calcein sticking to the cellular membrane and/or from endocytosis. In contrast, sonicated cells show a range of calcein uptake levels with a large group of intact, viable cells having background fluorescence similar to controls, another group having high fluorescence (high uptake), and a third group having low fluorescence (low uptake) in between. At 3.6 atm of ultrasound pressure, 10% of intact cells show low uptake and 10% show high uptake, and at 5.3 atm of ultrasound pressure, 15% of intact cells show low uptake and 24% show high uptake. This analysis allows us to distinguish between viable cells with background fluorescence (Population 1) and viable cells with elevated fluorescence indicating intracellular uptake (Population 2). The percentages of

all of the populations described above are compiled into the bar graph shown in Figure 3a.

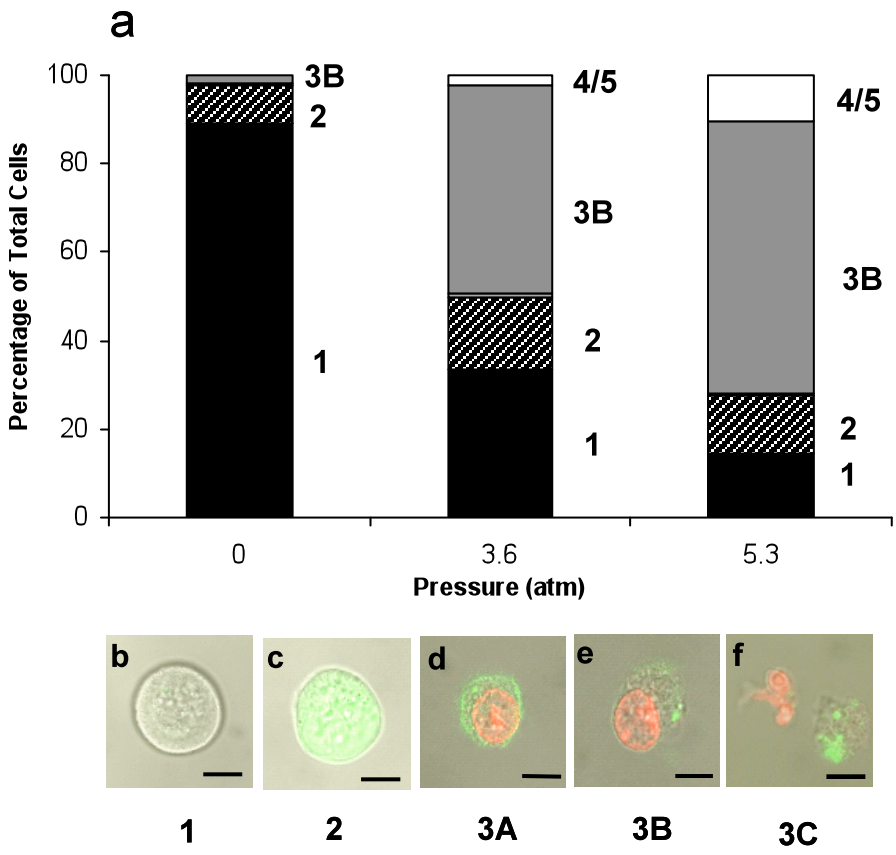

Figure 3. Cells are distributed across multiple populations after sonication. (a) A stacked bar graph shows a break down of the quantifiable populations. (b) An image of a cell sorted from viable populations (Populations 1 and 2) is shown to be unaffected by sonication. (c) A cell sorted from viable populations (Populations 1 and 2) shows intracellular calcein uptake (Population 2). (d) A cell sorted from Population 3 retains normal cellular size but has lost the ability to exclude PI (Population 3A). (e) A cell sorted from population 3 has an intact nucleus with plasma membrane remnants (Population 3B). (f) Cellular debris were collected by sorting all other populations.

4.4 Mechanical Sorting of Populations

To correlate our flow analysis with microscopy observations, we separated the cells into physical populations using a cell sorter based upon the gated populations of the analysis. Due to limitations of the instrument, we were able to

sort the samples using only two separate gates: events from Populations 1 and 2 in one gate and events from Populations 3A and 3B in the other. The debris populations (Populations 3C and 3D) were sorted by collecting all events not in these two gated regions. We then imaged the outputs from the sorting by confocal microscopy immediately after the samples were collected.

Representative images from sorting are shown in Figures 3b-f. Figures 3b and 3c show cells sorted from Populations 1 and 2. The cell in Figure 3b shows no obvious plasma membrane disruptions and no calcein uptake; therefore, this cell is consistent with our interpretation of Population 1 cells as unaffected. The cell in Figure 3c is also PI-negative, indicating an intact plasma membrane; however, this cell exhibits uptake of green-fluorescent calcein, signifying a repaired, transient membrane disruption and is consistent with Population 2 cell classification in our flow cytometric analysis.

The cells shown in Figures 3 d-f were sorted from Populations 3A, 3B and 3C. The cell shown in Figure 3d is similar in size to the cells from Population 1 but exhibits red PI fluorescence. Therefore, this cell would be classified as a Population 3A cell in our flow cytometric analysis. Figure 3e shows an intact nucleus that exhibits PI fluorescence and has remnants of disrupted plasma membrane as shown by the entrapment of calcein. These structures are representative of the wound-derived perikarya of Population 3B.

Figure 3f shows cellular debris sorted from Populations 3C and 3D. These debris consist of fragmented nuclei, organelles, and plasma membrane components; however, intact cells were no longer discernible in this image. The

representative populations obtained by sorting strengthen the validity of our flow cytometric analysis and provide a key link between quantifiable cellular characteristics and microscopy-observed cellular morphologies.

4.5 Significance

These results demonstrate the relative importance of the various ultrasound-induced bioeffects. Previously, these bioeffects were categorized in very general terms as uptake cells or dead cells. However, we have developed a means of measuring viability in a much more detailed manner. These new techniques allow us to understand the connection between the physical ultrasound conditions and the biological responses of the cells. By breaking the responses down into populations, we can begin to look at each population individually to determine methods to control the final cellular outcomes.

Chapter V

Analysis and Control of Ultrasound-Mediated Apoptosis

5.1 Introduction

Our previous analysis identified the cellular populations created immediately after sonication. A detailed and quantitative study of how cells may shift populations over time after sonication is lacking in the literature and therefore was the focus of our next analysis. If ultrasound is to be used for drug and gene delivery, it is necessary to understand the ultimate effects of ultrasound beyond the immediate consequences.

Our greatest concern was to track the movement of cells from Populations 1 and 2 into Population 3. We did not expect other shifts among populations because non-uptake cells (Population 1) were unlikely to become uptake cells (Population 2) well after sonication and non-viable cells (Population 3) were unlikely to become viable (Populations 1 and 2). However, cells that initially remained viable after sonication (Populations 1 and 2) could later lose viability (Population 3) as discussed in previous studies on ultrasound-induced apoptosis (Ashush, Rozenszajn et al. 2000; Lagneaux, de Meulenaer et al. 2002; Honda, Kondo et al. 2004; Feril, Kondo et al. 2005). We therefore monitored cells for 6 h after sonication, a time point previously identified as a maximum for early stages

of apoptosis caused by ultrasound (Feril, Kondo et al. 2004; Honda, Kondo et al. 2004).

5.2 Long-term Cell Death By Apoptosis

Figure 4 shows a breakdown of the two populations of cells initially classified as viable (Populations 1 and 2) after sonication. These two populations are shown as a percentage of intact cells and are distinguished by calcein fluorescence, indicating intracellular uptake in Population 2 cells. After 6 hours, the percentage of intact cells exhibiting intracellular uptake decreased by 15% in samples exposed to 5.3 atm of sonication pressure (Figure 3b, ANOVA $p < 0.05$). Correspondingly, the percentage of intact cells without calcein fluorescence increased by 15% in the same sonicated samples (Figure 4a). Since the overall percentage of intact cells (Populations 1 and 2) did not change over the 6 h period (data not shown), this indicates that a sizeable portion of uptake cells lost the ability to retain calcein (i.e. cells have shifted from Population 2 to Population 1) hours after sonication. Although the effect to cells in Population 2 appears initially to be reversible, this additional analysis shows that some cells have lasting effects that do not manifest themselves until hours later. When apoptotic pathways are initiated, cellular membranes can slowly become “leaky” (Darzynkiewicz, Bruno et al. 1992); therefore, intracellular calcein can diffuse out of the cells. We hypothesize that the delayed loss of cells in Population 2 is the result of apoptosis, possibly stimulated by the transient loss of plasma membrane integrity that initially permitted the entry of calcein into the cells.

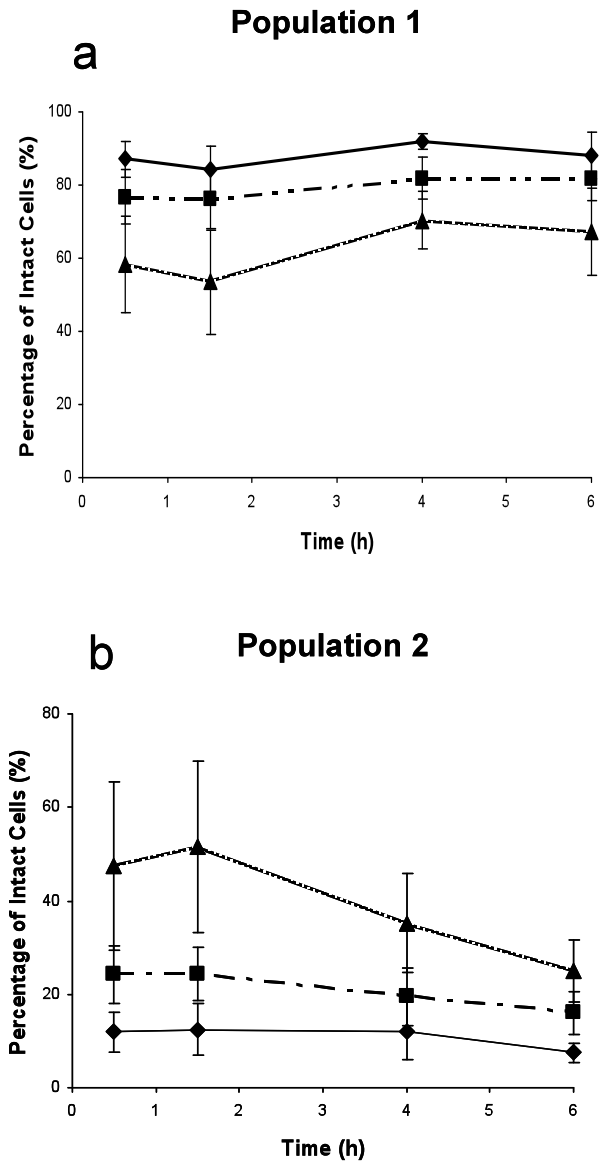

Figure 4. A separation of viable cells at three different conditions. Diamonds represent cells not exposed to ultrasound. Squares represent cells exposed to an ultrasound pressure of 3.6 atm. Triangles represent cells exposed to an ultrasound pressure of 5.3 atm. (a) Population 1 cells in samples exposed to 5.3 atm show a percentage increase after 6 h post-sonication. (b) Correspondingly, Population 2 cells in samples exposed to 5.3 atm show a quantifiable percentage decrease after 6 h post-sonication.

To test the hypothesis that DU145 cells die by apoptosis hours after ultrasound exposure, we used an annexin V assay as described in Chapter 3. All of the data presented were collected 6 hours post-sonication. Figures 5a-b show

the results of annexin V staining for a non-sonicated cell sample (Figure 5a) and a cell sample exposed to a sonication pressure of 5.3 atm at 6 hours post-sonication (Figure 5b). The quadrants were set based upon background fluorescence on non-sonicated samples. Cells in the lower left quadrant are normal viable cells. The upper right quadrant consists of cells that have lost plasma membrane integrity and is almost exclusively (95%) composed of cells from Population 3. Apoptotic cells show increased annexin V fluorescence but largely exclude PI and are grouped into the lower right quadrant of Figure 5b. At 6 hours after ultrasound exposure, 10% of intact cells for samples exposed to 3.6 atm of ultrasound pressure and 15% of intact cells for samples exposed to 5.3 atm of ultrasound pressure exhibit annexin V fluorescence and mostly exclude PI (Figure 5b, Lower Right Quadrant). The small increase in PI fluorescence shown by cells in this quadrant is most likely due to the leaky plasma membranes of early apoptotic cells. This observation is consistent with the loss of calcein from Population 2 cells as discussed in the previous section.

These results support the hypothesis that ultrasound induces apoptosis in sonicated cells hours after the initial exposure. A loss of cells from our desired population of uptake cells (Population 2) is of concern. We next sought to determine what caused some uptake cells to become apoptotic, with the goal that this insight could suggest strategies to “save” these cells and keep them from dying.

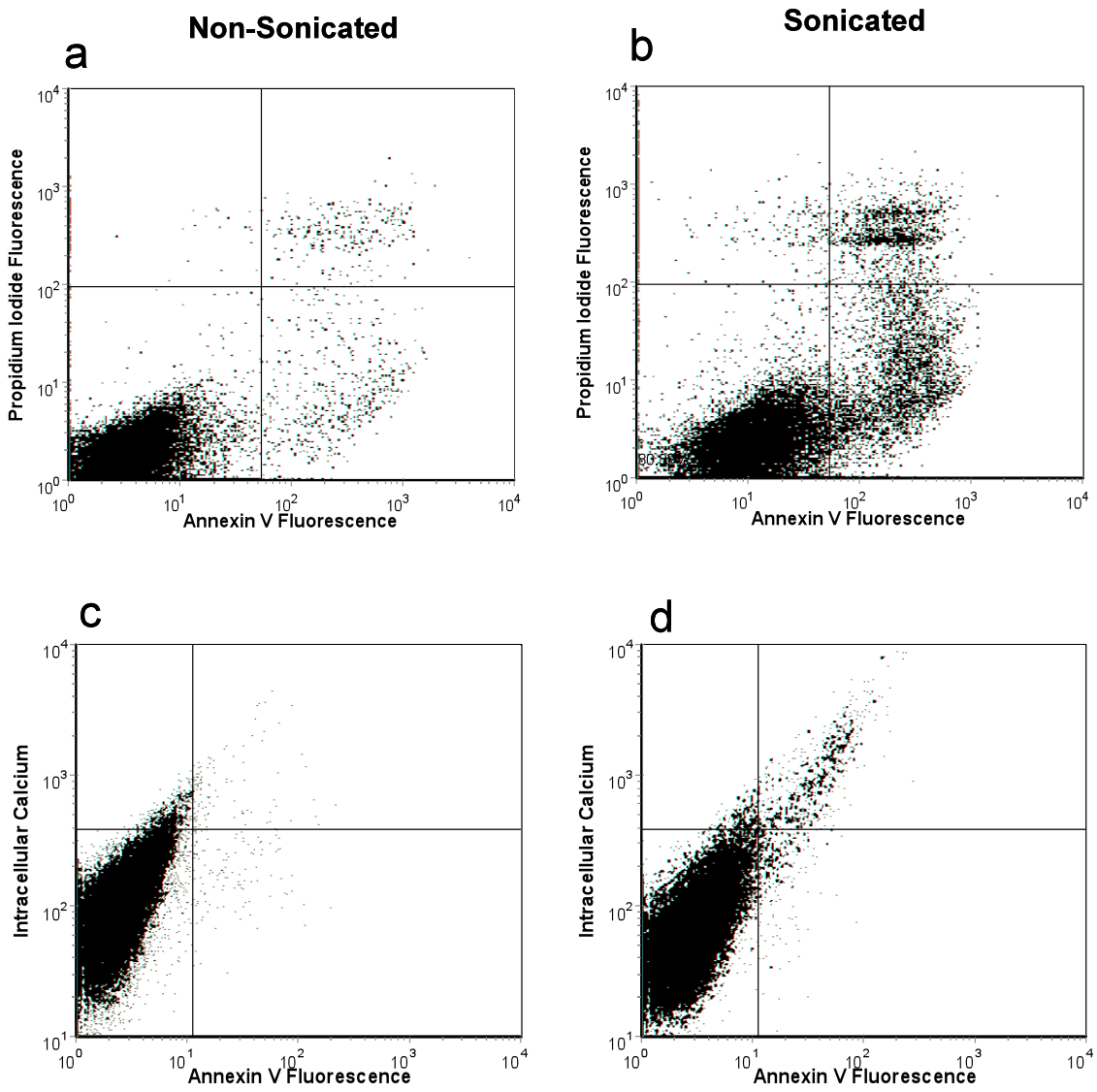

Figure 5. Flow cytometric dot plots connect apoptosis to increased intracellular Ca^{2+}. (a) Most non-sonicated cells are viable (PI-negative) and not undergoing apoptosis (annexin-positive). (b) At 6 h after ultrasound exposure, a sizeable number of cells are PI-negative but are in the early stages of apoptosis (annexin-positive). (c) Non-sonicated cells have background levels of Ca^{2+} fluorescence and are not undergoing apoptosis at 6 h post-sonication. (d) Most of the apoptotic cells in sonicated samples have higher levels of intracellular Ca^{2+}.

5.3 Ca^{2+} in Apoptotic Cells

The observed apoptosis occurred in samples sonicated in the presence of cellular growth medium in the absence of any assay markers. This technique ensures that the apoptosis was not caused by the presence of any assay

molecule alien to the cell and indicates that the apoptotic trigger did not originate from an influx of molecules and ions in the cellular growth medium. As mentioned previously, the onset of apoptosis after ultrasound exposure has been hypothesized to be a function of increased intracellular Ca^{2+} levels (Honda, Kondo et al. 2004). To determine whether ultrasound exposure resulted in increased intracellular Ca^{2+}, we used Fluo-4 AM, a Ca^{2+} specific fluorescent indicator, as described in Chapter 3. Figure 5c shows the results of this Ca^{2+} assay in a non-sonicated sample, and Figure 5d shows the change in Ca^{2+} and annexin V fluorescence in viable cells after an ultrasound exposure of 5.3 atm. All annexin-positive (i.e. apoptotic) cells also show an increase in intracellular Ca^{2+}, and all cells with the highest levels of intracellular Ca^{2+} exhibit annexin V fluorescence (Figure 5d, Upper Right Quadrant). This supports the hypothesis that ultrasound-induced apoptosis is associated with, and possibly initiated by, an increase in cytosolic Ca^{2+}. These results also suggest that cells that were initially classified as viable, uptake cells (Figure 2, Population 2) could be undergoing apoptosis hours after sonication due to a large influx of Ca^{2+} across the disrupted plasma membrane. When the ultrasonically-induced cavitation disrupts the plasma membrane of the cell and thereby permits entry of calcein molecules, the natural concentration gradient also causes extracellular Ca^{2+} ions to rush into the cell.

This suggests that viable uptake cells (Population 2) can die by apoptosis due to an influx of Ca^{2+} ions. However, the data indicate that a sizeable portion (approximately 20% of intact cells) of uptake cells retain calcein up to 6 hours

after sonication. This could imply that the initiation of apoptosis is sensitive to the level of Ca^{2+} loading. Based upon studies done on the link between Ca^{2+} and apoptosis, once a threshold concentration is reached, a cell may no longer be able to return to normal conditions (Berridge, Bootman et al. 1998; Nicotera and Orrenius 1998; Wertz and Dixit 2000; Orrenius, Zhivotovsky et al. 2003; Nguyen, Bittner et al. 2005). Uptake cells that do not reach this Ca^{2+} threshold may be able to recover and retain viability. We hypothesize that the level of intracellular Ca^{2+} loading is dependent upon the extent of plasma membrane wounding caused by ultrasound.

In order to relate the influx of Ca^{2+} to plasma membrane wounding (as indicated by calcein uptake), we plotted calcein uptake versus intracellular Ca^{2+} in viable cells. Figure 6 shows a representative plot of non-sonicated cells (Figure 6a) and of cells sonicated at 5.3 atm (Figure 6b). After sonication, essentially all cells with intracellular Ca^{2+} (> 99%) also exhibit calcein uptake (Figure 6b, upper-right quadrant). This supports the idea that the large increase in intracellular Ca^{2+} is a result of the same plasma membrane wounds that lead to calcein uptake. Furthermore, the level of intracellular Ca^{2+} corresponds well with the level of calcein uptake, and there is a high density region of cells at the highest Ca^{2+} loading (similar to the cells found to be annexin-positive in Figure 5d) corresponding to the highest calcein uptake (Figure 6b, arrow). For cells exposed to 3.6 atm of ultrasound pressure, approximately 7% of viable (PI-negative) cells can be grouped into this high density region, and for cells exposed to 5.3 atm of ultrasound pressure, approximately 12% of viable (PI-

negative) cells can be grouped into in this high density region. These percentages closely mirror the number of cells found to be apoptotic from the annexin results shown above.

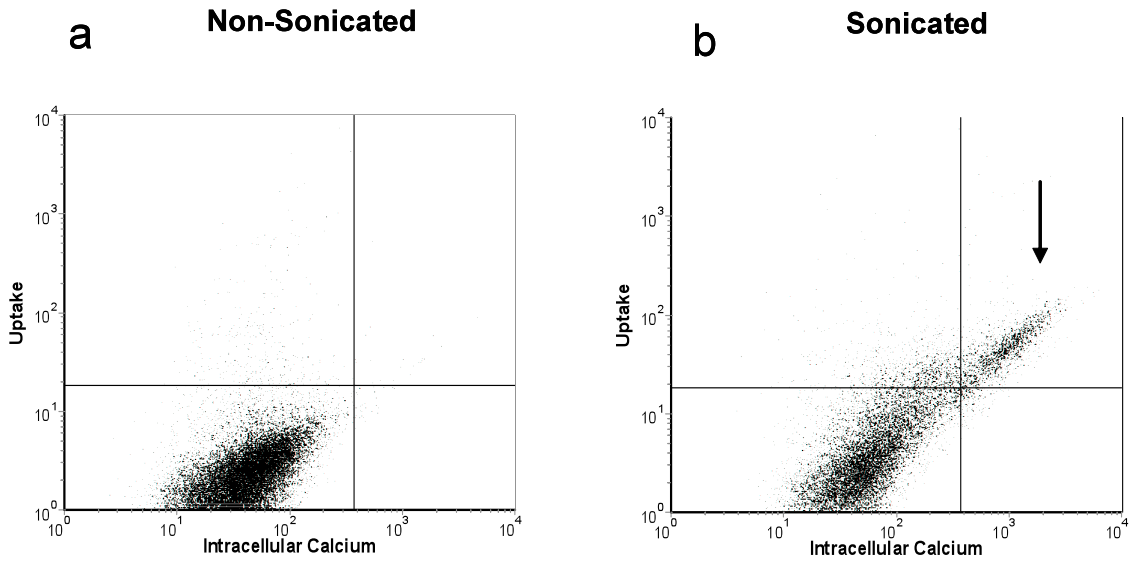

Figure 6. Intracellular Ca^{2+} versus calcein uptake. (a) Non-sonicated samples have background levels of intracellular Ca^{2+} and calcein fluorescence. (b) Sonicated cells show increased intracellular Ca^{2+} and calcein uptake. A high density population exists at the highest levels of both molecules (arrow).

Previous studies have indicated that the amount of cellular loading (i.e. the number of molecules per cell) caused by ultrasound varies within a sonicated sample (Cochran and Prausnitz 2001; Guzman, Nguyen et al. 2001; Keyhani, Guzman et al. 2001). The level of intracellular calcein fluorescence, an indicator of the number of molecules transported across the plasma membrane, corresponds to the wound size and the amount of time a cell was open to external molecules (i.e. the extent of plasma membrane wounding) (Zarnitsyn, Rostad et al. 2007). Therefore, cells with greater amounts of calcein uptake should also exhibit higher levels of intracellular Ca^{2+} since both molecules are

moving into the cell due to a concentration gradient between the cytosol and extracellular environment. If ultrasound-induced apoptosis is the result of an intracellular Ca^{2+} switch, there should be a threshold level of cellular wounding—as measured by calcein uptake—that leads to programmed cell death from an extracellular Ca^{2+} influx.

To study effects of the level of wounding on intracellular Ca^{2+} concentrations and ultrasound-induced apoptosis, we divided calcein uptake cells into two subpopulations—high uptake and low uptake (shown in Figure 2c-d). High uptake cells were chosen as those previously described as having "equilibrium loading" of calcein (Guzman, Nguyen et al. 2002); whereas, the low uptake population includes all cells with sub-equilibrium calcein loading. We then monitored these two populations over the course of 6 hours. The overall percentage of low uptake cells (Figure 7a) remains constant over time (ANOVA $p > 0.05$); whereas, the percentage of high uptake cells (Figure 7b) decreases over time (ANOVA $p < 0.05$).

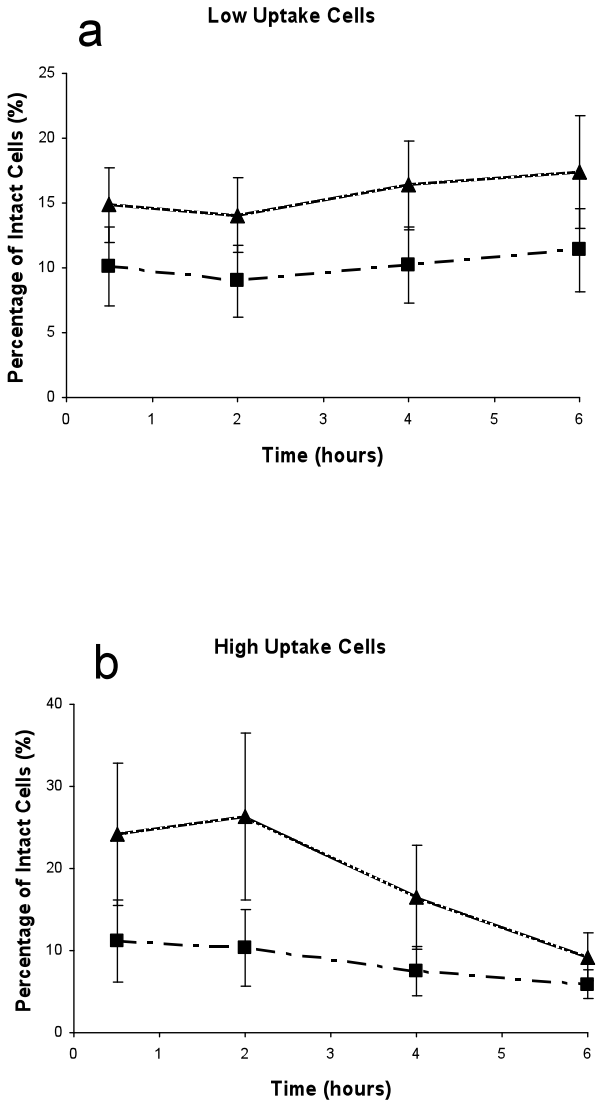

Figure 7. Uptake subpopulations over time. Squares represent samples exposed to 3.6 atm of ultrasound pressure, and triangles represent samples exposed to 5.3 atm ultrasound pressure. (a) The percentage of intact cells with low levels of calcein fluorescence does not change over the course of 6 hours. (b) However, at 5.3 atm high uptake cells show a quantifiable percentage decrease after 6 hours (ANOVA $p < 0.05$).

The observed percentage decrease of high uptake cells along with the increased concentration of intracellular Ca^{2+} in these cells suggests that these cells are annexin-positive apoptotic cells, as discussed previously. This relative correlation between apoptosis and uptake using Ca^{2+} as a link is necessary given

the limits of our flow cytometer and the fluorescent molecules available for the assays described above. Unfortunately, we were not able to make the connection directly; however, we feel that the data given strongly support this association.

5.4 Prevention of Apoptosis

Previous studies attempted to prevent apoptosis by chelating intracellular Ca^{2+} with BAPTA, AM, a Ca^{2+}-specific chelator for live cells, during sonication (Honda, Kondo et al. 2004). While this treatment was shown to prevent apoptosis, more cells died by necrosis (Population 3-type death) after sonication. The reason for the shift of cells from programmed cell death into uncontrolled modes of death can be explained by results found by Schlicher et. al. (Schlicher, Radhakrishna et al. 2006) and elsewhere in cellular wounding literature (Terasaki, Miyake et al. 1997; McNeil and Kirchhausen 2005). In these studies, Ca^{2+} was shown to be an important signaling molecule in cellular wound repair. In the absence of Ca^{2+}, cells cannot recruit lipid repair vesicles to the sites of plasma membrane disruption. Consequently, chelating Ca^{2+} in cells prior to or during sonication inhibits the ability of cells to recover normal membrane function after ultrasound exposure, and thus renders the cell non-viable. Other studies have indicated that Ca^{2+}-initiation of cellular wound repair occurs very rapidly; whereas, commencement of apoptosis may take up to minutes (Berridge, Bootman et al. 1998). These results indicate an opportunity to allow cells to repair and save cells from apoptosis by chelating intracellular Ca^{2+} shortly after sonication.

Therefore, to save cells from apoptosis we added BAPTA, AM 1 min after sonication. Within 2 hours after chelation, Ca^{2+} levels were reduced in all cells as shown in Figure 8a. Furthermore, the number of apoptotic cells is decreased by approximately 50% at both ultrasound pressures 6 hours after sonication (Figure 8b). By chelating the intracellular Ca^{2+} after sonication, we believe that wound-repair mechanisms were initiated, and therefore, uptake (Figure 8c) and short-term cellular viability (Figure 8d) were not affected by the BAPTA, AM treatment but apoptosis was still often averted. This indicates that Population 2 cells were saved and remained viable up to 6 hours after sonication.

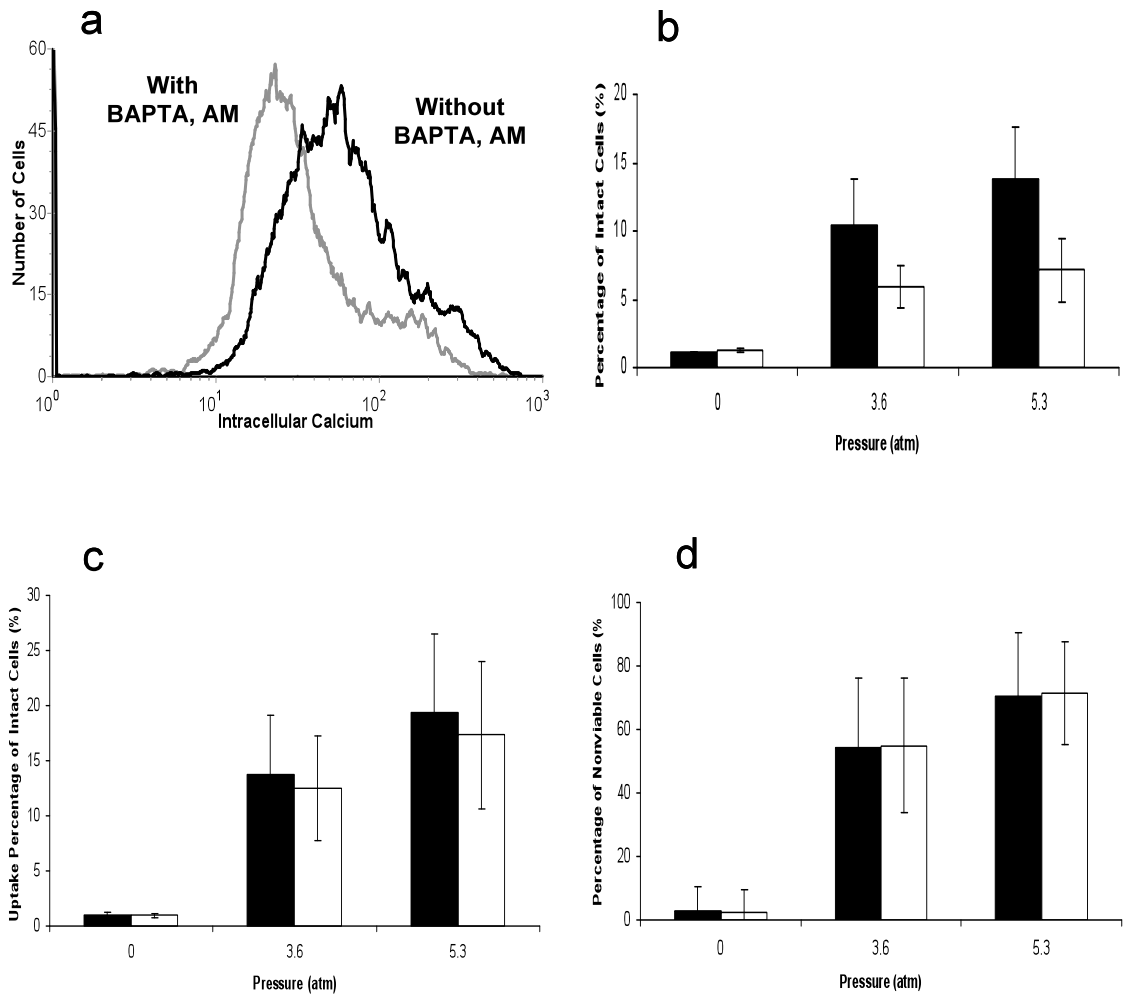

Figure 8. The effects of Ca^{2+} chelation with BAPTA, AM. For the bar graphs, the black bars represent samples without BAPTA, AM and the white bars represent samples with BAPTA, AM. (a) BAPTA, AM chelates Ca^{2+} in all cells. The black line shows cells without BAPTA, AM and the gray line shows cells with BAPTA, AM. (b) Apoptosis is decrease by 50% of intact cells following intracellular Ca^{2+} chelation. (c) The percentage of uptake cells remain unchanged after post-sonication Ca^{2+} chelation. (d) Rapid viability losses are not changed after post-sonication Ca^{2+} chelation.

5.5 Significance

These results show that Ca^{2+} is a key mediator of ultrasound-induced apoptosis. We were able to use flow cytometry to connect the increase intracellular Ca^{2+} to an influx of external molecules following plasma membrane wounding. Since Ca^{2+} is required to initiate plasma membrane repair, we added

BAPTA, AM, an intracellular Ca^{2+} chelator, after sonication, allowing time for activation of wound repair pathways. We have shown that this chelation method can save cells from ultrasound-mediated apoptosis.

Chapter VI

Discussion

6.1 Identification of Cellular Outcomes

We have shown that there are three primary cellular outcomes immediately after sonication: 1) cells are unaffected by ultrasound; 2) cells are opened temporarily to allow for intracellular transport and then subsequently resealed; 3) cells are rendered non-viable by ultrasound. Using flow cytometry, we correlated these scenarios to characteristic cellular populations. For application purposes, maximizing the number of viable cells with intracellular uptake (Population 2) and minimizing the number of non-viable cells (Population 3) is desirable.

By monitoring these populations over the course of 6 h, we noticed that a subset of Population 2 cells, corresponding to those cells with the highest levels of intracellular uptake, were lost. Since the proposed purpose of this research is to use ultrasound as a drug delivery method, the conclusion that ultrasonically-induced delivery of external molecules causes a loss of cellular viability within 6 h post-sonication is counter to the goal of using ultrasound as a clinical tool. Therefore, we wanted to understand why these cells became apoptotic so that we could try to intervene. Insight from previous studies led us to monitor levels of intracellular Ca^{2+} as a possible mediator of apoptosis. Our Ca^{2+} assays

revealed that the intracellular Ca^{2+} concentrations in sonicated cells were increased beyond the normal levels present in cytosolic homeostasis and intracellular stores. In this way, we found that intracellular Ca^{2+} levels correlated with intracellular levels of our model drug, calcein indicating that these cells were reversibly permeabilized by the ultrasonically induced cavitation. This suggested that the desired effect of drug uptake was directly tied to the undesired effect of Ca^{2+} uptake that caused apoptosis.

Previous studies have identified a heterogeneity in the levels of uptake in sonicated cells (Guzman, Nguyen et al. 2001; Keyhani, Guzman et al. 2001). Therefore, we wanted to look more closely at the relationship between the levels of calcein uptake and ultrasound-induced apoptosis. The fact that some uptake cells are able to remain viable throughout the timeframe studied suggested that a threshold intracellular Ca^{2+} concentration could be responsible for the observed apoptosis, and that this concentration is strongly dependent upon the size of the ultrasound-mediated wounds in the plasma membranes of the cells.

These results also explain the difference in apoptotic cell death at the two sonication pressures studied. Samples exposed to ultrasound at 5.3 atm have a significantly higher portion of uptake cells (22% of intact cells) in the high uptake range than samples exposed to ultrasound at 3.6 atm (11% of intact cells), and as a result, a significantly higher portion of cells exposed to the higher sonication pressure undergo apoptosis than cells exposed to the lower sonication pressure. The increased number of permeabilized cells led to more cells with a Ca^{2+} concentration above the apoptotic threshold. However, since the amount

delivered to cells is less at lower ultrasound pressures, it is often desirable to use higher pressure conditions. Our work showed, however, that this approach to increase uptake can be counter productive, due to the associated increase in apoptosis.

6.2 Ca^{2+} Chelation Prevents Apoptosis

Many apoptotic inhibition techniques may be effective in preventing ultrasound-induced apoptosis. Apoptotic signaling pathways can be very complex, involving the activation and regulation of many different enzymes in parallel. Therefore, it is often desirable to inhibit apoptosis by targeting the point of apoptotic initiation, thereby avoiding the intricate pathways. For the purposes of these studies, Ca^{2+} chelation was chosen due to the belief that the influx of the Ca^{2+} ions into the cells was an initial apoptotic trigger. However, since the repair of cellular membranes has also been shown to be mediated by Ca^{2+} signaling, we had to take into account the relative biochemical dynamics of apoptotic and plasma membrane repair.

The sensitivity of Ca^{2+}-mediated biochemical signaling is dependent on both the concentration of the Ca^{2+} as well as the amount of time an increased level of Ca^{2+} exists in the cell (Berridge, Bootman et al. 1998). By understanding the concentration and temporal limits for intracellular Ca^{2+} in both cellular wound repair and programmed cell death, we can significantly alter cellular outcomes. While previous studies (Honda, Kondo et al. 2004) correctly identified Ca^{2+} as an important mediator of ultrasound-induced apoptosis, Ca^{2+} chelation during sonication resulted in uncontrolled viability loss. An increase in intracellular Ca^{2+}

is needed to initiate plasma membrane wound repair (Terasaki, Miyake et al. 1997; McNeil and Kirchhausen 2005); however, by chelating the Ca^{2+} with BAPTA, AM 1 min post-sonication, wound-repair pathways are able to proceed, but apoptotic signaling pathways are alleviated. This allowed us to reduce the number of apoptotic cells without forcing cells into uncontrolled, necrotic death. The reduced levels of apoptosis after the Ca^{2+} chelation treatment also strengthen the hypothesis that an influx of external Ca^{2+} leads to apoptosis after ultrasound exposure.

6.3 Modeling Gives Insight Into Wound Severity

We have connected ultrasound-induced apoptosis to a large Ca^{2+} influx resulting from plasma membrane breaches that also lead to equilibrium loading of model drug molecules, such as calcein. This connection allows us to use a molecular flux model developed by Zarnitsyn et. al. (Zarnitsyn, Rostad et al. 2007) to approximate the minimum level of plasma membrane wounding that leads to sufficient Ca^{2+} influx to cause apoptosis. This model was created to capture the dynamics of plasma membrane wound repair after sonication and in this way, predicts plasma membrane wound size as a function of intracellular uptake of calcein. By integrating the flux equation to time at infinity (after the plasma membrane is completely repaired), the following relationship is obtained:

$$Q(\infty) = C_o K R_o t_{rel}, \qquad (1)$$

where Q is the total amount of calcein in a cell, C_o is the initial concentration of calcein outside of the cell, R_o is the initial radius of the plasma membrane wound, t_{rel} is the characteristic relaxation time of the system, and K is a relationship of calcein diffusivities in cellular cytosol ($D_{\alpha,cyt}$) and water (D_α) given below.

$$K = \frac{4D_{\alpha}}{\left(1 + \frac{D_{\alpha}}{D_{\alpha,cyt}}\right)} \quad \textbf{(2)}$$

The total amount of calcein inside cells (molecules per cell) was found using methods described in Chapter 3. The external calcein concentration was known, and the relaxation time and diffusivities were assumed to be constant and used as noted by Zarnitsyn. Therefore, the initial radius of the ultrasound-induced plasma membrane wound can be found from Equation 1. Although this is a first order model of plasma membrane wounding, it offers useful insight into the relative wound severity leading to specific bioeffects.

Zarnitsyn found that cells were no longer able to repair plasma membrane wounds with radii above 300 nm (Zarnitsyn, Rostad et al. 2007). This means that the first wave of ultrasound-induced viability loss occurs during, or shortly after, sonication when wounds are greater than 300 nm. Desirable wounds that lead to calcein uptake are repaired within 10 min after sonication has ended (Schlicher, Radhakrishna et al. 2006). However, as we have shown, at a certain uptake threshold, cells will become apoptotic hours after sonication. The radius leading to this amount of uptake was calculated using Equation 1 where Q was found by quantifying the number of molecules per cell in the high uptake population (established in Figure 2). According to the model, short-term uptake can occur through cellular membrane wounds with radii up to 300 nm; however, after approximately 4 hours post-sonication, cells with wounds that initially had radii larger than 90 nm begin to die by apoptosis. For cells to retain uptake molecules for the duration of this study, the initial wound radii had to be less than 90 nm.

Figure 9 shows a schematic of the possible cellular outcomes post-sonication. The vertical axis indicates the relative severity of ultrasound-derived cellular wounds that lead to the various outcomes. The values shown are derived from the model discussed above. The horizontal axis indicates the timeline of cellular bioeffects occurring from sonication. These values are based upon experimental observations. From this diagram, we can establish windows within which ultrasound can be an effective drug delivery device.

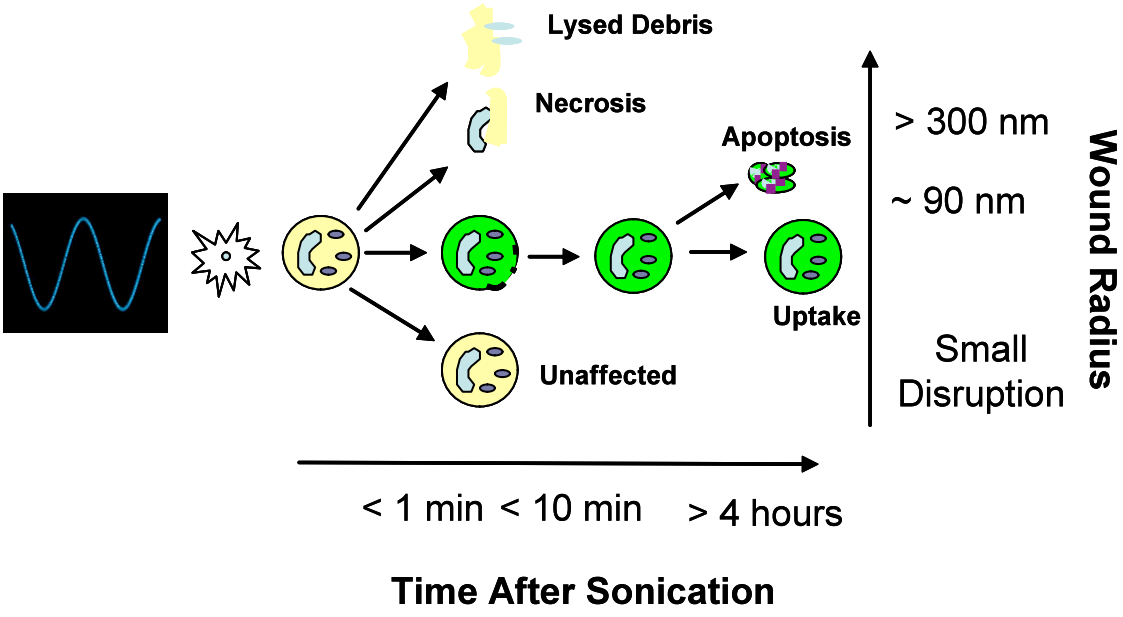

Figure 9. Schematic showing cellular outcomes as a function of time after sonication and plasma membrane wound radius.

6.4 Treatment Strategies

By chelating intracellular Ca^{2+} after sonication, we have shown the ability to save cells that would originally have died hours after ultrasound exposure. Since more cells are now able to maintain viability after ultrasound, we have effectively increased the "size" of allowable plasma membrane disruptions as discussed in the model above. This is especially beneficial in therapeutics

requiring the delivery of large molecules such as DNA, RNA, and proteins. For example, this treatment has the potential to significantly increase transfection efficiencies for ultrasound gene delivery because more cells would survive the large wounds needed to deliver DNA into the cytosol. Clinically, this type of treatment could be realized by injecting a drug or therapeutic molecule into a patient, sonicating at the target site, and then adding an intracellular Ca^{2+} chelator shortly after sonication.

Chapter VII

Conclusions

Ultrasound has potential as a non-invasive drug delivery device; however, its clinical application has been hampered by a lack of predictability and controllability. The first objective of this study was to characterize and quantify ultrasound-mediated bioeffects. We have shown that the heterogeneous effects of ultrasound can be quantified by flow cytometric analytical methods. Our analysis provides key insight into the relative importance of rapid cell death events by grouping cells into characteristic populations. We then monitored the shift in these populations at two sonication pressures to gain a better understanding of the role of ultrasound in causing different types of rapid cell death. We found that an increase in pressure causes more severe death effects (i.e. cellular lysis) but that at both pressures considered the majority of rapid death was resulted in a necrotic death mode creating cellular structures previously termed wound-derived perikarya. Identifying these death modes could shed light on future methods to control ultrasound-induced rapid viability losses.

Secondly, we were also interested in understanding the long-term effects of ultrasound to cells initially characterized as viable after sonication. Consistent with previous observations, we found that a significant portion of cells exhibited signs of programmed cell death 6 h after sonication; however, we were able to

connect this cell death to a loss of cellular homeostasis resulting from an influx of extracellular Ca^{2+} through the same large plasma membrane disruptions that cause high levels of intracellular uptake. This connection led us to our last objective of controlling the downstream effects of ultrasound.

By identifying Ca^{2+} as a key apoptotic mediator, we hypothesized that intracellular Ca^{2+} chelation could allow us to prevent apoptosis. However, since Ca^{2+} is an important signaling molecule in cellular wound repair and apoptosis, saving apoptotic cells by Ca^{2+} chelation had to be done after sonication. The initial rush of Ca^{2+} ions into wounded cells allowed the activation of plasma membrane repair pathways to occur, but by removing the Ca^{2+} shortly after the end of sonication, we were able to prevent the onset of apoptosis. Therefore, we increased the overall viability of sonicated samples up to 6 h after sonication.

Our findings offer promise toward the eventual control of ultrasound-mediated bioeffects. We have shown that short-term viability losses can be grouped into characteristic populations and are a function of ultrasound pressure. We have also demonstrated that long-term viability losses may be prevented by early intervention strategies to help the cells cope with the effects of plasma membrane wounding. These conclusions suggest that all ultrasound-induced viability losses are a function of the initial wound to the cellular membranes. Therefore, the key to controlling the bioeffects caused by ultrasound may lie in controlling these wounds.

Chapter VIII

Recommendations

The findings of this work lead to a host of interesting studies that could help further the ultimate goal of using ultrasound as a drug delivery device. The observation that post-sonication Ca^{2+} chelation can prevent ultrasound-induced apoptosis is extremely important, and therefore, more work should be done optimizing this technique. Optimization parameters include the concentration of the chelator and the post-sonication time of chelation. Through this optimization, valuable biochemical information can also be obtained. For example, since one molecule of BAPTA, AM is responsible for sequestering one Ca^{2+} ion, the relationship between chelator concentration and apoptosis prevention also gives insight into the critical Ca^{2+} concentrations that lead to programmed cell death. This information could also be used to validate the Zarnitsyn model presented in Chapter 6. A known concentration of intracellular Ca^{2+} can be connected to a Ca^{2+} flux into the cells—similar to the flux of calcein into the cell used for the model. Also, by understanding the effects of Ca^{2+} chelation and various times after sonication, we can begin to elucidate the kinetics of the activation of wound repair and apoptotic pathways. These techniques and results would be valuable not only to ultrasound research, but to any broad areas of research concerned with the affects of cellular wounding.

Along with studies into Ca^{2+}-mediated apoptosis, we should also be concerned with the effects of other molecules entering and leaving the cells during plasma membrane disruption. Ca^{2+} is an important signaling molecule, but there are many other extracellular molecules that can also impact cellular behavior when plasma membrane function is lost. Loss of cellular homeostasis could continue to affect cells after sonication and could contribute to a significant portion of the apoptosis that we have not been able to prevent through our chelation techniques.

While this study has the potential to solve the long-term viability problem, a majority of cell death is due to rapid losses of viability. As we have shown, rapid death populations can be partially controlled by changing the ultrasound conditions—namely, ultrasound peak pressure and exposure time. More rigorous studies should be done to understand the types of wounds that lead to short-term viability losses. Ideally, we want to shift all cells into the viable uptake population (Population 2). To do this, we need a better understanding of the physical mechanism of ultrasound that leads to the desired cellular effects. One method of doing this would be to use a microdevice in which the location of cavitation can be varied relative to cells. Using developed cavitation models, we could then gain insight into the interplay between cavitational forces and cellular responses that lead to the various populations described in this study. This could lead to a more rational ultrasound design that could create the appropriate “type” of cavitation.

Recent studies in our lab have found that exposure to infrared lasers can also deliver molecules into cells without the rapid viability losses observed in ultrasound (Chakravarty 2007). Since the amount of molecules delivered to cells is similar to the quantities observed using ultrasound, this treatment would probably cause long-term viability losses as described in Chapter 5. Therefore, we could combine our treatment with the laser therapy to create a treatment with minimal viability losses and high uptake. We may also be able to incorporate lessons learned from mechanistic studies on the function of laser-mediated drug delivery into our ultrasound delivery system.

Once we have optimized our system, an important step would be to demonstrate the effectiveness of the treatment in an animal model. It is necessary to show that the lessons learned on cells in vitro can be extended into living tissues. The ultimate goal of this research is to develop a delivery device that could be used in a clinical setting. Achievement of this goal could be realized through the studies discussed above.

References

Ariuens, E. J. and A. M. Simonis (1964). "A Molecular Basis for Drug Action. the Interaction of One or More Drugs with Different Receptors." J Pharm Pharmacol **16**: 289-312.

Ashush, H., L. A. Rozenszajn, et al. (2000). "Apoptosis Induction of Human Myeloid Leukemic Cells by Ultrasound Exposure." Cancer Research **60**: 1014-1020.

Barnett, S. B., G. R. ter Haar, et al. (1994). "Current status of research on biophysical effects of ultrasound." Ultrasound Med Biol **20**(3): 205-18.

Bednarski, M. D., J. W. Lee, et al. (1997). "In vivo target-specific delivery of macromolecular agents with MR-guided focused ultrasound." Radiology **204**(1): 263-8.

Berridge, M. J., M. D. Bootman, et al. (1998). "Calcium--a life and death signal." Nature **395**(6703): 645-8.

Bohm, I. and H. Schild (2003). "Apoptosis: The Complex Scenario for a Silent Cell Death." Molecular Imaging and Biology **5**(1): 2-14.

Burek, C. J., M. Burek, et al. (2003). "Calcium induces apoptosis and necrosis in hematopoetic malignant cells: Evidence for caspase-8 dependent and FADD-autonomous pathway." Gene Therapy and Molecular Biology **7**: 173-179.

Campbell, P. and M. R. Prausnitz (2007). "Future directions for therapeutic ultrasound." Ultrasound Med Biol **33**(4): 657.

Canatella, P. J., M. M. Black, et al. (2004). "Tissue electroporation: quantification and analysis of heterogeneous transport in multicellular environments." Biophys J **86**(5): 3260-8.

Canatella, P. J., J. F. Karr, et al. (2001). "Quantitative study of electroporation-mediated molecular uptake and cell viability." Biophys J **80**(2): 755-64.

Carstensen, E. L., P. Kelly, et al. (1993). "Lysis of erythrocytes by exposure to CW ultrasound." Ultrasound Med Biol **19**(2): 147-65.

Chakravarty, P. (2007). Personal Communication. J. D. Hutcheson. Atlanta, GA.

Cochran, S. A. and M. R. Prausnitz (2001). "Sonoluminescence as an indicator of cell membrane disruption by acoustic cavitation." Ultrasound Med Biol **27**(6): 841-50.

Cupp, C. L. and D. C. Bloom (2002). "Gene therapy, electroporation, and the future of wound-healing therapies." Facial Plast Surg **18**(1): 53-7.

Dalecki, D. (2004). "Mechanical Bioeffects of Ultrasound." Annual Review of Biomedical Engineering **6**: 229-248.

Dalecki, D., C. H. Raeman, et al. (1997). "Remnants of Albunex nucleate acoustic cavitation." Ultrasound Med Biol **23**(9): 1405-12.

Darzynkiewicz, Z., S. Bruno, et al. (1992). "Features of apoptotic cells measured by flow cytometry." Cytometry **13**(8): 795-808.

Duvshani-Eshet, M., L. Baruch, et al. (2006). "Therapeutic ultrasound-mediated DNA to cell and nucleus: bioeffects revealed by confocal and atomic force microscopy." Gene Ther **13**(2): 163-72.

Duvshani-Eshet, M. and M. Machluf (2005). "Therapeutic ultrasound optimization for gene delivery: a key factor achieving nuclear DNA localization." J Control Release **108**(2-3): 513-28.

Edinger, A. L. and C. B. Thompson (2004). "Death by design: apoptosis, necrosis and autophagy." Curr Opin Cell Biol **16**(6): 663-9.

Fadeel, B., B. Zhivotovsky, et al. (1999). "All along the watchtower: on the regulation of apoptosis regulators." The FASEB Journal **13**: 1647-1657.

Feril, J., Loreto B., T. Kondo, et al. (2004). "Enhanced ultrasound-induced apoptosis and cell lysis by a hypotonic medium." International Journal of Radiation Biology **80**(2): 165-175.

Feril, L. B., Jr., T. Kondo, et al. (2005). "Apoptosis induced by the sonomechanical effects of low intensity pulsed ultrasound in a human leukemia cell line." Cancer Lett **221**(2): 145-52.

Gac, S. L., E. Zwaan, et al. (2007). "Sonoporation of suspension cells with a single cavitation bubble in a microfluidic confinement." Lab Chip **7**(12): 1666-72.

Guzman, H. R., A. J. McNamara, et al. (2003). "Bioeffects caused by changes in acoustic cavitation bubble density and cell concentration: a unified explanation based on cell-to-bubble ratio and blast radius." Ultrasound Med Biol **29**(8): 1211-22.

Guzman, H. R., D. X. Nguyen, et al. (2001). "Ultrasound-mediated disruption of cell membranes. I. Quantification of molecular uptake and cell viability." J Acoust Soc Am **110**(1): 588-96.

Guzman, H. R., D. X. Nguyen, et al. (2001). "Ultrasound-mediated disruption of cell membranes. II. Heterogeneous effects on cells." J Acoust Soc Am **110**(1): 597-606.

Guzman, H. R., D. X. Nguyen, et al. (2002). "Equilibrium Loading of Cells with Macromolecules by Ultrasound: Effects of Molecular Size and Acoustic Energy." Journal of Pharmaceutical Sciences **91**(7): 1693-1701.

Hallow, D. M., A. D. Mahajan, et al. (2007). "Ultrasonically targeted delivery into endothelial and smooth muscle cells in ex vivo arteries." J Control Release **118**(3): 285-93.

Honda, H., T. Kondo, et al. (2004). "Role of Intracellular Calcium Ions and Reactive Oxygen Species in Apoptosis Induced by Ultrasound." Ultrasound in Medicine and Biology **30**(5): 683-692.

Honda, H., Q. L. Zhao, et al. (2002). "Effects of dissolved gases and an echo contrast agent on apoptosis induced by ultrasound and its mechanism via the mitochondria-caspase pathway." Ultrasound Med Biol **28**(5): 673-82.

Husseini, G. A., R. I. El-Fayoumi, et al. (2000). "DNA damage induced by micellar-delivered doxorubicin and ultrasound: comet assay study." Cancer Lett **154**(2): 211-6.

Kamaev, P. P., J. D. Hutcheson, et al. (2004). "Quantification of optison bubble size and lifetime during sonication dominant role of secondary cavitation bubbles causing acoustic bioeffects." J Acoust Soc Am **115**(4): 1818-25.

Keyhani, K., H. R. Guzman, et al. (2001). "Intracellular Drug Delivery Using Low-Frequency Ultrasound: Quantification of Molecular Uptake and Cell Viability." Pharmaceutical Research **18**(11): 1514-1520.

Kinoshita, M. and K. Hynynen (2005). "A novel method for the intracellular delivery of siRNA using microbubble-enhanced focused ultrasound." Biochem Biophys Res Commun **335**(2): 393-9.

Kitanaka, C. and Y. Kuchino (1999). "Caspase-independent programmed cell death with necrotic morphology." Cell Death Differ **6**(6): 508-15.

Ko, K. S. and C. A. McCulloch (2000). "Partners in protection: interdependence of cytoskeleton and plasma membrane in adaptations to applied forces." J Membr Biol **174**(2): 85-95.

Kroemer, G., B. Dallaporta, et al. (1998). "The Mitochondrial Death/Life Regulator in Apoptosis and Necrosis." Annual Review of Physiology **60**: 619-642.

Lagneaux, L., E. C. de Meulenaer, et al. (2002). "Ultrasonic low-energy treatment: a novel approach to induce apoptosis in human leukemic cells." Exp Hematol **30**(11): 1293-301.

Langer, R. (1998). "Drug delivery and targeting." Nature **392**(6679 Suppl): 5-10.

Lauterborn, W. and C. D. Ohl (1997). "Cavitation bubble dynamics." Ultrason Sonochem **4**(2): 65-75.

Leighton, T. G. (2007). "What is ultrasound?" Prog Biophys Mol Biol **93**(1-3): 3-83.

Love, R. R., H. Leventhal, et al. (1989). "Side effects and emotional distress during cancer chemotherapy." Cancer **63**(3): 604-12.

Marin, A., H. Sun, et al. (2002). "Drug delivery in pluronic micelles: effect of high-frequency ultrasound on drug release from micelles and intracellular uptake." J Control Release **84**(1-2): 39-47.

McNeil, P. L. and T. Kirchhausen (2005). "An emergency response team for membrane repair." Nat Rev Mol Cell Biol **6**(6): 499-505.

McNeil, P. L., K. Miyake, et al. (2003). "The endomembrane requirement for cell surface repair." Proc Natl Acad Sci U S A **100**(8): 4592-7.

McNeil, P. L. and R. A. Steinhardt (1997). "Loss, restoration, and maintenance of plasma membrane integrity." J Cell Biol **137**(1): 1-4.

McNeil, P. L., S. S. Vogel, et al. (2000). "Patching plasma membrane disruptions with cytoplasmic membrane." Journal of Cell Science **113**: 1891-1902.

Mehier-Humbert, S., T. Bettinger, et al. (2005). "Plasma membrane poration induced by ultrasound exposure: implication for drug delivery." J Control Release **104**(1): 213-22.

Meldolesi, J. (2003). "Surface wound healing: a new, general function of eukaryotic cells." J Cell Mol Med **7**(3): 197-203.

Miller, D. L. and J. Quddus (2001). "Lysis and sonoporation of epidermoid and phagocytic monolayer cells by diagnostic ultrasound activation of contrast agent gas bodies." Ultrasound Med Biol **27**(8): 1107-13.

Miller, M. W., D. L. Miller, et al. (1996). "A review of in vitro bioeffects of inertial ultrasonic cavitation from a mechanistic perspective." Ultrasound Med Biol **22**(9): 1131-54.

Morris, C. E. and U. Homann (2001). "Cell surface area regulation and membrane tension." J Membr Biol **179**(2): 79-102.

Ng, K. Y. and Y. Liu (2002). "Therapeutic ultrasound: its application in drug delivery." Med Res Rev **22**(2): 204-23.

Nguyen, M. P., G. D. Bittner, et al. (2005). "Critical interval of somal calcium transient after neurite transection determines B 104 cell survival." J Neurosci Res **81**(6): 805-16.

Nicotera, P., G. Bellomo, et al. (1990). "The role of Ca2+ in cell killing." Chem Res Toxicol **3**(6): 484-94.

Nicotera, P. and S. Orrenius (1998). "The role of calcium in apoptosis." Cell Calcium **23**(2/3): 173-180.

Ogawa, K., K. Tachibana, et al. (2001). "High-resolution scanning electron microscopic evaluation of cell-membrane porosity by ultrasound." Med Electron Microsc **34**(4): 249-53.

Ogawa, R., G. Kagiya, et al. (2004). "Ultrasound mediated intravesical transfection enhanced by treatment with lidocaine or heat." J Urol **172**(4 Pt 1): 1469-73.

Orrenius, S., B. Zhivotovsky, et al. (2003). "Regulation of Cell Death: The Calcium-Apoptosis Link." Nature Reviews Molecular Cell Biology **4**: 552-565.

Paliwal, S. and S. Mitragotri (2006). "Ultrasound-induced cavitation: applications in drug and gene delivery." Expert Opin Drug Deliv **3**(6): 713-26.

Postema, M. and O. H. Gilja (2007). "Ultrasound-directed drug delivery." Curr Pharm Biotechnol **8**(6): 355-61.

Pouton, C. W. and L. W. Seymour (2001). "Key issues in non-viral gene delivery." Adv Drug Deliv Rev **46**(1-3): 187-203.

Proskuryakov, S. Y., V. L. Gabai, et al. (2002). "Necrosis Is an Active and Controlled Form of Programmed Cell Death." Biochemistry (Moscow) **67**(4): 467-491.

Rettig, J. and E. Neher (2002). "Emerging roles of presynaptic proteins in Ca++-triggered exocytosis." Science **298**(5594): 781-5.

Rosenthal, I., J. Z. Sostaric, et al. (2004). "Sonodynamic therapy--a review of the synergistic effects of drugs and ultrasound." Ultrason Sonochem **11**(6): 349-63.

Schlicher, R. K., J. D. Hutcheson, et al. (2007). Georgia Institute of Technology.

Schlicher, R. K., H. Radhakrishna, et al. (2006). "Mechanism of intracellular delivery by acoustic cavitation." Ultrasound Med Biol **32**(6): 915-24.

Sundaram, J., B. R. Mellein, et al. (2003). "An experimental and theoretical analysis of ultrasound-induced permeabilization of cell membranes." Biophys J **84**(5): 3087-101.

Tang, H., C. C. Wang, et al. (2002). "An investigation of the role of cavitation in low-frequency ultrasound-mediated transdermal drug transport." Pharm Res **19**(8): 1160-9.

ter Haar, G. (2007). "Therapeutic applications of ultrasound." Prog Biophys Mol Biol **93**(1-3): 111-29.

Terasaki, M., K. Miyake, et al. (1997). "Large Plasma Membrane Disruptions Are Rapidly Resealed by Ca2+-dependent Vesicle-Vesicle Fusion Events." The Journal of Cell Biology **139**(1): 63-74.

Trump, B. F. and I. K. Berezesky (1992). "The role of cytosolic Ca2+ in cell injury, necrosis and apoptosis." Curr Opin Cell Biol **4**(2): 227-32.

Trump, B. F. and I. K. Berezesky (1995). "Calcium-mediated cell injury and cell death." The FASEB Journal **9**: 219-228.

Trump, B. F., I. K. Berezesky, et al. (1997). "The pathways of cell death: oncosis, apoptosis, and necrosis." Toxicol Pathol **25**(1): 82-8.

Tsong, T. Y. (1991). "Electroporation of cell membranes." Biophys J **60**(2): 297-306.

Tsujimoto, Y. (1997). "Apoptosis and necrosis: intracellular ATP level as a determinant for cell death modes." Cell Death Differ **4**(6): 429-34.

Vlahakis, N. E. and R. D. Hubmayr (2000). "Invited review: plasma membrane stress failure in alveolar epithelial cells." J Appl Physiol **89**(6): 2490-6;discussion 2497.

Vykhodtseva, N., N. McDannold, et al. (2001). "Apoptosis in ultrasound-produced threshold lesions in the rabbit brain." Ultrasound Med Biol **27**(1): 111-7.

Weaver, J. C. (1993). "Electroporation: a general phenomenon for manipulating cells and tissues." J Cell Biochem **51**(4): 426-35.

Wertz, I. E. and V. M. Dixit (2000). "Characterization of calcium release-activated apoptosis of LNCaP prostate cancer cells." J Biol Chem **275**(15): 11470-7.

Zamansky, G. B., U. Nguyen, et al. (1991). "An immunofluorescence study of the calcium-induced coordinated reorganization of microfilaments, keratin intermediate filaments, and microtubules in cultured human epidermal keratinocytes." J Invest Dermatol **97**(6): 985-94.

Zarnitsyn, V. G., P. P. Kamaev, et al. (2007). "Ultrasound-enhanced chemotherapy and gene delivery for glioma cells." Technol Cancer Res Treat **6**(5): 433-42.

Zarnitsyn, V. G., C. M. Rostad, et al. (2007). "Modeling of transmembrane transport through cell membrane wounds following acoustic cavitation." Biophys J **Submitted**.